Model Identity S_N2 Reactions $CH_3X + X^-$ (X = F, Cl, CN, OH, SH, NH_2, PH_2): Marcus Theory Analyzed

Jason M. Gonzales, Wesley D. Allen, and Henry F. Schaefer III*

Center for Computational Chemistry, University of Georgia, Athens, Georgia 30602-2525

Received: August 22, 2005

The structures of seven gas phase identity S_N2 reactions of the form $CH_3X + X^-$ have been characterized with seven distinct theoretical methods: RHF, B3LYP, BLYP, BP86, MP2, CCSD, and CCSD(T), in conjunction with basis sets of double and triple ζ quality. Additionally, the energetics of said reactions have been definitively computed using focal point analyses utilizing extrapolation to the one-particle limit for the Hartree−Fock and MP2 energies using basis sets of up to aug-cc-pV5Z quality, inclusion of higher order correlation effects [CCSD and CCSD(T)] with basis sets of aug-cc-pVTZ quality, and additional auxiliary terms for core correlation and scalar relativistic effects. Final net activation barriers for the reactions are $E^b_{F,F} = -0.8$, $E^b_{Cl,Cl} = 1.6$, $E^b_{CN,CN} = 28.7$, $E^b_{OH,OH} = 14.3$, $E^b_{SH,SH} = 13.8$, $E^b_{NH_2,NH_2} = 28.6$, and $E^b_{PH_2,PH_2} = 25.7$ kcal mol^{-1}. General trends in the energetics, specifically the performance of the density functionals, and the component energies of the focal point analyses are discussed. The utility of classic Marcus theory as a technique for barrier predictions has been carefully analyzed. The standard Marcus theory results show disparities of up to 9 kcal mol^{-1} with respect to explicitly computed results. However, when alternative approaches to Marcus theory, independent of the well-depths, are considered, excellent performance is achieved, with the largest deviations being under 3 kcal mol^{-1}.

Introduction

Bimolecular nucleophilic substitution (S_N2) reactions at carbon centers are among the most studied of all chemical reactions. Early research into this most fundamental class of organic reactions was in the solution phase, but advances in the 1970s in flowing afterglow[1−3] and ion-cyclotron resonance[4−6] techniques later spawned an interest in the gas phase chemistry of these reactions, where intrinsic reactivity can be ascertained and solvent effects exposed. Gas phase S_N2 reactions have been found to generally have a classic double-well potential with a central inversion barrier. For an identity gas phase S_N2 reaction, the energy profile is shown in Figure 1, where E^w is the ion−molecule complexation energy, E^b is the net activation barrier, and E^* is the central activation barrier. The myriad investigations of gas phase S_N2 reactions include a variety of kinetics experiments,[3,4,7−14] quantum and semiclassical dynamical studies and trajectory simulations,[15−22] statistical mechanical analyses,[5,23−28] ab initio and density functional electronic structure theory,[29−45] and electron transfer studies.[46−51] The preponderance of S_N2 studies in the chemical literature has made these reactions a paradigm for ion−molecule reactions in general.

There have been two previous high level theoretical studies of nonidentity reactions of the type $CH_3X + F^-$ (X = F, Cl, CN, OH, SH, NH_2, PH_2).[44,45] These investigations were designed to obtain definitive structural and energetic data for these seven reactions[45] and to assess and calibrate density functional theory for S_N2 systems.[44] Here, we undertake detailed analyses of the associated identity exchange reactions $CH_3X + X^-$ (X = F, Cl, CN, OH, SH, NH_2, PH_2), obtaining well-converged ab initio energetics, in most cases for the first time. With our highly accurate, explicitly computed barriers, we then analyze Marcus theory[52,53] as a simple means of predicting and rationalizing the energetics of S_N2 reactions. Some of the nonidentity reactions studied in the earlier research do not have intrinsic reaction paths exhibiting classic backside attack and thus do not fit neatly into the scheme of Figure 1. Therefore, we additionally explore the use of backside structures optimized with the constraint of linear X−C−Y frameworks as reference geometries for defining central S_N2 barriers. In such cases, a key question is which definition of the central barrier (frontside or backside) is more appropriate for organizing principles such as Marcus theory.

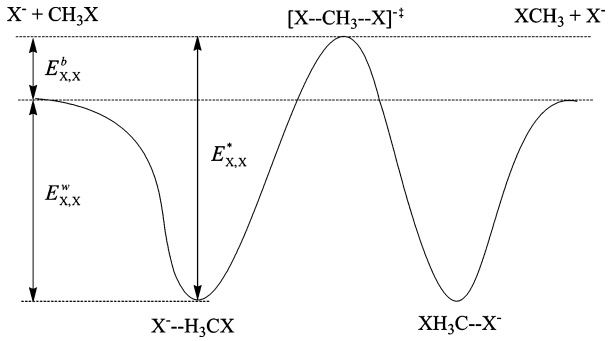

Figure 1. Energy diagram for a prototypical gas phase identity S_N2 reaction. Note the double well with two minima corresponding to ion−molecule complexes.

Marcus theory has its origins in the investigations of electron transfer reactions in solution.[52,53] Marcus derived a simple expression, which related the activation energy of these reactions to the overall thermodynamics. In search of rate−equilibrium relationships, which have long intrigued chemists, the original work of Marcus was extended to proton transfer reactions,[54,55] hydrogen transfer reactions,[56,57] and of course methyl transfer

* To whom correspondence should be addressed. E-mail: hfs@uga.edu.

10.1021/jp054734f CCC: $30.25
Published on Web 10/28/2005

reactions.[24−26,58−62] In the Marcus expression, the activation energy (E^*) for an elementary process is essentially partitioned into thermodynamic and kinetic components:

$$E^* = E_0^* + \frac{\Delta E}{2} + \frac{(\Delta E)^2}{16E_0^*} \quad (1)$$

where ΔE is the reaction energy and E_0^* is a hypothetical intrinsic barrier devoid of a thermodynamic driving force. In the direct application of eq 1 to a gas phase S_N2 reaction, ΔE and E^* are the energies of the product ion−molecule complex and the S_N2 transition state, respectively, relative to the reactant ion−molecule complex. To obtain a relationship for the overall activation energy of the complete reaction going from separated reactants to separated products, additional assumptions are required,[26,58] or ion−molecule binding energies must be known.

Identity reactions play a key role in Marcus theory because they provide a $\Delta E = 0$ reference point for which the central barrier and the intrinsic barrier are the same. In his original work,[63] Marcus proposed the additivity postulate

$$E_0^*(\mathrm{X,Y}) = \frac{E_0^*(\mathrm{X,X}) + E_0^*(\mathrm{Y,Y})}{2} \quad (2)$$

which, if applied to a crossed S_N2 reaction involving nucleophile X and leaving group Y, means that the intrinsic barrier in eq 1 should be taken as the average of the corresponding barriers for the X and Y identity exchange reactions. Prior work by Wladkowski and Brauman[62] has shown the consistency of the additivity postulate. According to eqs 1 and 2, if the barriers for a set of identity exchange reactions are known, then the barriers for all cross-reactions within the group may be readily estimated from the corresponding reaction energies alone. In 1981, Wolfe, Mitchell, and Schlegel[58,64] found a high correlation between S_N2 barriers estimated via the Marcus approach and explicitly computed ab initio results, but at the time, only a modest level of theory was feasible (RHF/4-31G).

Over two decades of dramatic advances in theoretical methodology and computational hardware have made it possible to now converge ab initio reaction energies and central barriers of model S_N2 reactions to near chemical accuracy (1 kcal mol^{-1}) or better. For identity exchange reactions, the only prior work that can be said to be of chemical accuracy is limited to the halogen systems, namely, $CH_3F + F^-$,[33,42−45] $CH_3Cl + Cl^-$,[37,42,43] and $CH_3Br + Br^-$.[42,43] This dearth was a key motivation for us to execute careful computational studies to expand the number of identity reactions characterized to true chemical accuracy or better. As a fruit of this effort, an assessment of the validity of Marcus theory for S_N2 reactions can be made for the first time with definitive energetic data.

In our previous work,[45,65] we reviewed some of the plentiful model chemistries[66] available for refining ab initio energetic predictions. The Gaussian-*n* (G1, G2, G3, and variants) methods of Pople, Raghavachari, Curtiss, and others[67−71] are some of the most popular and widely applicable among such techniques. A similar approach is found in the CBS-*n* procedures developed by Petersson et al.[72−74] The major difference with respect to the Gaussian-*n* model chemistries is the extrapolation of the MP2 energy using the CBS2 procedure.[75] Previous benchmarking shows similar performance for CBS-Q and G2.[73] Both the CBS-*n* and the Gaussian-*n* procedures resort to some level of empirical correction to achieve mean target accuracies of 1−2 kcal mol^{-1}. Another black-box model chemistry are the W1−W4 schemes of Martin et al.[76,77] These methods attempt to systematically converge to the ab initio limit by extrapolating Hartree−Fock, CCSD, and CCSD(T) energies for W1 and W2, while adding extrapolations for CCSDT and CCSDTQ levels for W3 and W4, respectively. Future revisions of W4 are planned to include extrapolations up to CCSDTQ5 and include corrections for Born−Oppenheimer breakdown. Finally, corrections for auxiliary effects such as core correlation and special relativity are included. W1 has one empirical parameter for the exponent of extrapolation of the CCSD and CCSD(T) energies, while W2−W4 have no empirical character. In principle, these methods, particularly W2−W4, are capable of surpassing chemical accuracy in the energetics. As in the Gaussian-*n* and CBS-*n* cases, there are variants of W1−W4 that modify the refinement process.

The thermochemical refinement scheme utilized in this paper is the focal point method, developed by Allen and coworkers[33,45,65,78−80] and summarized in the next section. The focal point method is not a model chemistry in that it avoids universal, black-box prescriptions in order to retain the flexibility to achieve the best possible, fully ab initio predictions for a given chemical system. In addition to extrapolating to complete basis set and high-order electron correlation limits, the method accounts for core correlation,[78,81−86] relativistic effects,[87−92] and non-Born−Oppenheimer terms. The technical goal of the focal point analyses performed here is to determine the critical energetic quantities for the (X = F, Cl, CN, OH, SH, NH_2, PH_2) identity S_N2 reactions to subchemical accuracy

$$E_{\mathrm{X,X}}^{\mathrm{w}} = E(\mathrm{X}^- \cdot \mathrm{CH_3X}) - E(\mathrm{CH_3X}) - E(\mathrm{X}^-) \quad (3)$$

$$E_{\mathrm{X,X}}^{\mathrm{b}} = E[(\mathrm{X - CH_3 - X})^{-\ddagger}] - E(\mathrm{CH_3X}) - E(\mathrm{X}^-) \quad (4)$$

$$E_{\mathrm{X,X}}^{*} = E[(\mathrm{X - CH_3 - X})^{-\ddagger}] - E(\mathrm{X}^- \cdot \mathrm{CH_3X}) \quad (5)$$

These results will then be conjoined with the earlier definitive results[45] for $CH_3X + F^-$ (X = F, Cl, CN, OH, SH, NH_2, PH_2) to analyze the Marcus theory.

Computational Methods

Seven distinct theoretical methods were utilized for geometry optimizations and harmonic vibrational frequencies for this paper. They include four ab initio methods, restricted Hartree−Fock (RHF), second-order Møller−Plesset perturbation theory (MP2),[93] and coupled cluster theory including single and double excitations (CCSD),[94−96] as well as a perturbative contribution for connected triples [CCSD(T)].[97] Three density functional methods (B3LYP, BLYP, and BP86) were also employed in this investigation. The B3LYP functional is a combination of the hybrid three-parameter Becke exchange functional (B3)[98] and the Lee−Yang−Parr correlation functional (LYP).[99] The BLYP functional is a pure DFT method using the exchange functional of Becke (B)[100] with the Lee−Yang−Parr correlation functional (LYP). The BP86 functional is also a pure DFT method using the exchange functional of Becke (B) and the correlation functional of Perdew (P86).[101]

The basis sets utilized for the geometry optimizations were the DZP+dif, TZ2P+dif, and TZ2Pf+dif sets described in detail in our prior work.[44] All RHF, DFT, and MP2 computations utilized analytic first and second derivatives to obtain optimum geometries and harmonic vibrational frequencies, respectively. Coupled cluster geometry optimizations also utilized analytic first derivatives. All structures were tightly converged, with maximum residual Cartesian forces in the 10^{-5} to 10^{-6} hartree bohr^{-1} range. In the MP2 geometry optimizations, core orbitals

were frozen (but no virtuals deleted), while no orbitals were excluded in the coupled cluster correlation treatments.

Final results for the key energetic quantities defined in Figure 1 were obtained with the focal point method of Allen and co-workers,[33,45,65,78−80] as described below. Principally, the aug-cc-pV*X*Z basis sets of Dunning and co-workers[102−107] were employed. Because a tight *d* function may be necessary to describe core polarization effects in second-row atoms,[108−111] we performed additional studies with the recently developed aug-cc-pV(*X*+*d*)Z basis sets of Dunning et al.[112]

In the notation of the focal point analyses, ΔE denotes a relative energy for a chemical process, whereas δ signifies an incremental change in ΔE with respect to the preceding level of theory in a defined correlation sequence; thus, $\Delta E(\mathrm{CCSD}) = \Delta E(\mathrm{MP2}) + \delta(\mathrm{CCSD})$, for example. The energy data in each focal point decomposition are all based on a common reference geometry, the CCSD(T)/TZ2Pf+dif optimized structure in almost all cases. The two exceptions here are the ion−molecule complexes of the $X = NH_2$ and PH_2 systems, for which CCSD(T)/TZ2P+dif optimized geometries were used due to size and symmetry constraints. Focal point analyses are performed on the valence electron correlation problem first, and core correlation effects are included after the valence limit is inferred. Details of the focal point procedure utilized in this work are as follows.

(i) The RHF energy is extrapolated according to the three-parameter form[113] $E_{\mathrm{RHF}}(X) = E^{\infty}_{\mathrm{RHF}} + ae^{-bX}$, where X is the cardinal number in the aug-cc-pV*X*Z basis sets. The reaction energy at the Hartree−Fock limit ($\Delta E_{\mathrm{RHF}}{}^{\infty}$) is computed using these extrapolated values in eqs 3−5. For the second-row systems containing Cl, S, and P, comparative extrapolations using the aug-cc-pV(*X*+*d*)Z basis sets were performed. Although RHF energies were determined for $X = 2-5$, only the TZ-5Z values were included in the extrapolations, due to the generally poor performance of the aug-cc-pVDZ basis.

(ii) The MP2 correlation energy is extrapolated according to the two-parameter form[79,80] $E_{\mathrm{MP2}}(X) - E_{\mathrm{SCF}}(X) = \epsilon^{\infty}_{\mathrm{MP2}} + bX^{-3}$. From the extrapolated complete basis set MP2 correlation energy ($\epsilon^{\infty}_{\mathrm{MP2}}$), the second-order correlation increment to the relative energy is computed, $\delta(\mathrm{MP2}^{\infty}) = \Delta E^{\infty}_{\mathrm{MP2}} - \Delta E^{\infty}_{\mathrm{RHF}}$. Once again, TZ-5Z aug-cc-pV*X*Z energies were employed in the fit, and additional aug-cc-V(*X*+*d*)Z extrapolations were performed for the systems containing second-row atoms.

(iii) Basis set effects for the coupled cluster correlation energies are assumed to be additive. Accordingly, the increments $\delta(\mathrm{CCSD}) = \Delta E_{\mathrm{CCSD}} - \Delta E_{\mathrm{MP2}}$ and $\delta[(\mathrm{T})] = \Delta E_{\mathrm{CCSD(T)}} - \Delta E_{\mathrm{CCSD}}$ to the relative energies are computed with the aug-cc-pVTZ [and in second-row cases the aug-cc-pV(T+*d*)Z] basis set in this investigation. The additivity principle rests in the consistent observation[33,45,65,80] that the CCSD−MP2 and CCSD(T)−CCSD increments to the relative energies converge rapidly as X increases in the aug-cc-pV*X*Z series, facilitating high accuracy predictions even when aug-cc-pVQZ and aug-cc-pV5Z coupled cluster calculations are prohibitively large.

(iv) Unscaled MP2/TZ2Pf+dif harmonic vibrational frequencies are used to compute the zero-point vibrational energy contributions, $\Delta(\mathrm{ZPVE})$.

(v) The effects of core correlation, $\Delta(\mathrm{CC})$, on relative energies are evaluated at the MP2 level with basis sets of aug-cc-pCV*X*Z quality. For first-row atoms, the aug-cc-pCV*X*Z basis sets[106] are well-established, but at the beginning of this project, the analogous basis sets had not yet been established for second-row atoms. Thus, in the present research, we created custom basis sets, designated as aug-CV(T+*d*)Z, for Cl, S, and P, following a well-established procedure.[84,114] This construction entailed a complete uncontraction of the *sp* space of the aug-cc-pV(T+*d*)Z basis set, followed by augmentation with a tight 2*d*2*f* set, whose exponents were obtained by even-tempered extension into the core with a geometric ratio of 3. For hydrogen, the aug-cc-pVTZ basis set was used in evaluations of $\Delta(\mathrm{CC})$. In our prior work,[45] CCSD(T) was the method utilized for the explicit computation of $\Delta(\mathrm{CC})$ for S_N2 energetics, but we found that the average MP2 disparity vis-à-vis CCSD(T) for the core correlation shift was only 0.037 kcal mol^{-1}, the largest deviation being 0.125 kcal mol^{-1}. This calibration justifies the use of MP2 results for the largest systems studied here, where unfrozen core CCSD(T)/aug-cc-pCVTZ computations are not feasible.

(vi) Scalar relativistic effects, $\Delta(\mathrm{Rel})$, arising from the one-electron Darwin and mass-velocity operators, are accounted for using CCSD(T)/TZ2P+dif density matrices via the formalism of Perera and Bartlett.[89,91,92]

(vii) The final extrapolated focal point results (ΔE_{fp}) for the energetic quantities of eqs 3−5 are obtained as

$$\Delta E_{\mathrm{fp}} = \Delta E^{\infty}_{\mathrm{RHF}} + \delta(\mathrm{MP2}^{\infty}) + \delta(\mathrm{CCSD}) + \delta[(\mathrm{T})] + \Delta(\mathrm{ZPVE}) + \Delta(\mathrm{CC}) + \Delta(\mathrm{Rel}) \quad (6)$$

No corrections were made for basis set superposition error. For the Hartree−Fock and MP2 energies, because we are extrapolating to the complete basis limit, it should not be an issue. For the other corrections, the careful design of the correlation consistent basis sets should preclude this from being important.

The general RHF, DFT, and MP2 optimizations and vibrational frequencies (for all basis sets) were computed with the Gaussian 94[115] package. All coupled cluster optimizations were completed with the ACESII software suite. For the focal point analyses, ACESII was utilized for the aug-cc-pVDZ calculations, NWChem 4.1[116] for the aug-cc-pVTZ calculations, and PSI 3.0[117] for the aug-cc-pVQZ and aug-cc-PV5Z calculations. The auxiliary corrections were all computed with the ACESII package.

Results

A. Geometric Structures. Before the energetics of the six S_N2 reactions can be discussed, it is necessary to analyze the attendant structures. Optimizations were performed with seven methods [RHF, B3LYP, BLYP, BP86, MP2, CCSD, and CCSD(T)] and three basis sets (DZP+dif, TZ2P+dif, and TZ2Pf+dif). For brevity, we present only the RHF, B3LYP, MP2, and CCSD(T) TZ2Pf+dif results, as variability with respect to basis sets is small. We will focus attention mostly on the definitive CCSD(T) structures, pointing out discrepancies with the lower levels of theory when appropriate. The complete set of data is available in the Supporting Information.

It is first illustrative to analyze the structures of the reaction $CH_3F + F^-$, shown in Figure 2. This is an immensely popular reaction for study,[29,31−33,42−45,61,118−121] which has been analyzed with very high levels of theory. These include the original focal point work of Wladkowski et al.,[33] the QCISD(T) work of Lee et al.,[43] and the W2 extrapolation of Parthiban et al.[42] This reaction exhibits what will be referred to as classic S_N2 character. This categorization requires a linear (i.e., linear with respect to the three heavy atoms) backside complex, which appears to be a charge−dipole interaction. The large F−C distance of 2.575 Å is consistent with this type of interaction. The transition state displays full D_{3h} symmetry, with elongated F−C lengths of 1.826 Å. For this particular case, there is good

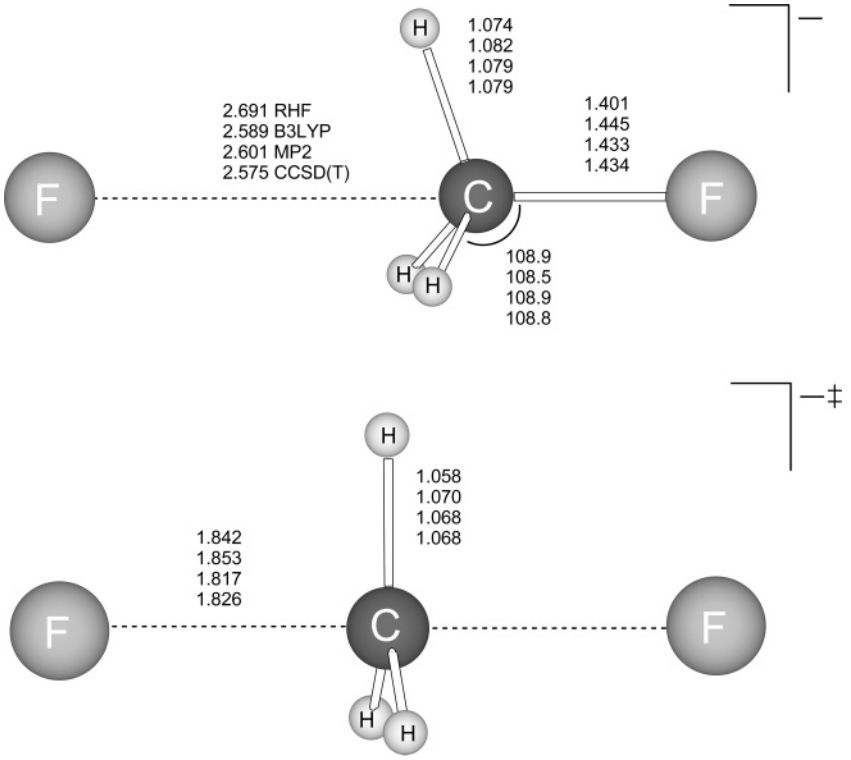

Figure 2. Geometries of the ion−molecule complex and transition state for the reaction $CH_3F + F^-$ using the TZ2Pf+dif basis set. All bond distances are in angstroms, and bond angles are in degrees. The ion−molecule complex is in C_{3v} symmetry while the transition state is in D_{3h} symmetry.

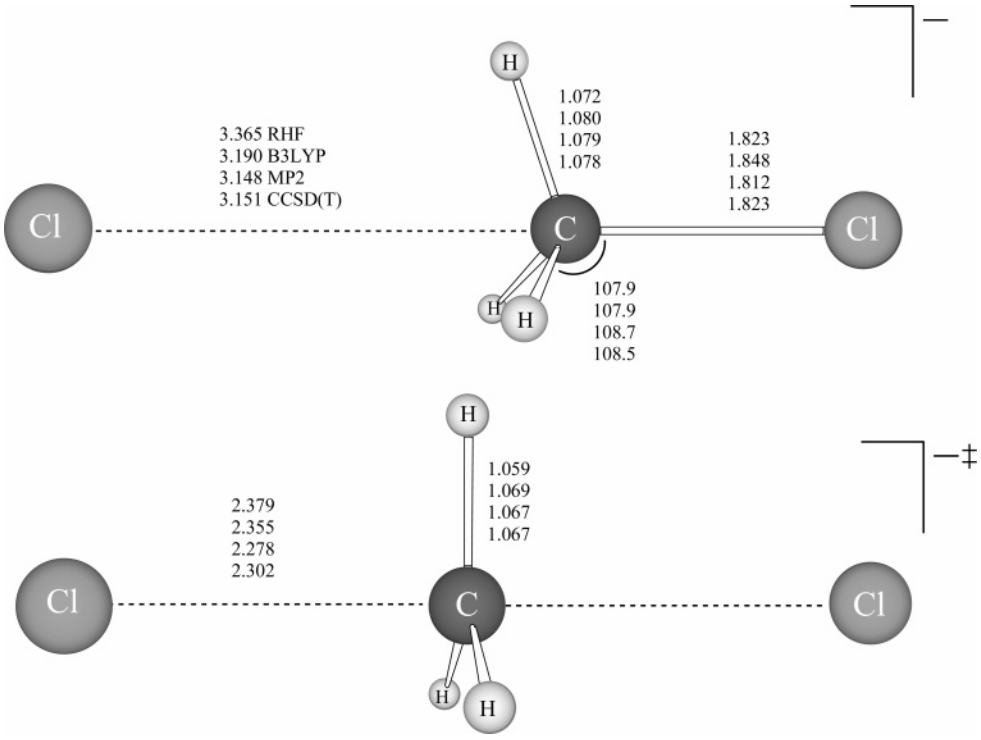

Figure 3. Geometries of the ion−molecule complex and transition state for the reaction $CH_3Cl + Cl^-$ using the TZ2Pf+dif basis set. All bond distances are in angstroms, and bond angles are in degrees. The ion−molecule complex is in C_{3v} symmetry while the transition state is in D_{3h} symmetry.

agreement among the correlated and density functional methods and between the current geometries and the results of prior research.

We begin the present analysis with the identity reaction $CH_3Cl + Cl^-$, with the ion−molecule complex and transition state shown in Figure 3. Along with the fluoride identity reaction, this is among the most studied of all S_N2 reactions.[16,18,29,32,61,118,121−125] The best previous studies have utilized CCSD(T),[37] QCISD(T),[43] and the W2[42] extrapolation schemes. The ion−molecule complex is a classic backside complex, in C_{3v} symmetry, with collinear heavy atoms and a large Cl−C distance of 3.151 Å. This structure is consistent with the classic

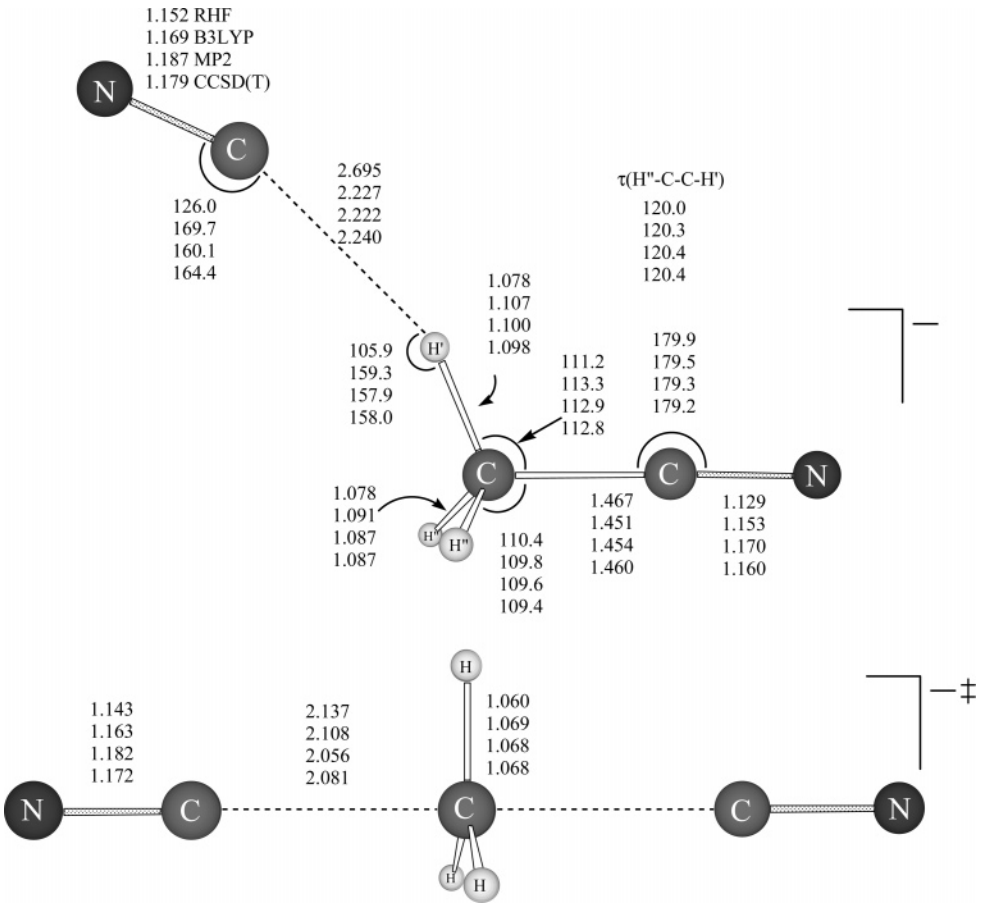

Figure 4. Geometries of the ion−molecule complex and transition state for the reaction $CH_3CN + CN^-$ using the TZ2Pf+dif basis set. All bond distances are in angstroms, and bond angles are in degrees. The ion−molecule complex is in C_s symmetry, while the transition state is in D_{3h} symmetry. The notation of this and all subsequent figures has H as a nonmethyl hydrogen, H′ as the unique methyl hydrogen, and H″ as one of the symmetry equivalent methyl hydrogens.

charge-permanent dipole structures characterized in similar structures.[45] The transition state, in D_{3h} symmetry, is also collinear with extended C−Cl bond lengths of 2.302 Å. For these two structures, the DFT and ab initio structures are in good agreement with one minor B3LYP deviation of roughly 0.05 Å in the long bond distances. In all cases, the present geometries are in good agreement with previous computations.

Figure 4 illustrates the ion−molecule complex and transition state associated with the reaction $CH_3CN + CN^-$. The only prior work on this identity reaction is the exploration of backside barriers performed by Uggerud[10] and an analysis of the kinetic isotope effect conducted by Ruggiero and Williams.[126] The ion−molecule complex, in C_s symmetry, is backside, but not collinear. Essentially, the NC^- anion is attracted to a unique methyl hydrogen, with a slight distortion of the acetonitrile moiety. The distance between the cyanide anion and the methyl hydrogen is 2.240 Å. This is almost 1 Å shorter than the long bond in $Cl^-\cdots H_3Cl$. This may indicate some small semicovalent character (as was found for $F^-\cdots CH_3CN$), but this is unlikely due to the very extended length. The transition state, in D_{3h} symmetry, has all heavy atoms collinear. In this case, the C−C bond distance is 2.081 Å. In all cases, there is excellent agreement among the present DFT and ab initio methods and the prior work mentioned.

The situation grows more complex for the $CH_3OH + OH^-$ identity reaction, as shown in Figure 5. The only prior work on this reaction is an analysis of the reaction profile performed by Uggerud.[10] Unfortunately, he considered only backside structures, so no direct comparison with our complex (which is not backside) is possible. As was previously shown in the reaction of $CH_3OH + F^-$,[44,45,127] nucleophiles can be attracted to the acidic hydrogen on methanol. In the $CH_3OH + OH^-$ case, the hydroxyl has started to abstract the acidic hydrogen, forming a relatively short O−H bond of just over an angstrom, while the methoxy O−H bond is 1.417 Å by comparison. Note the small torsional angle between the abstracted hydrogen and one of the methyl hydrogens. This is the exact opposite of what was observed for the $CH_3OH + F^-$ reaction, in which the fluoride anion is anti to the symmetry unique methyl hydrogen. In the $CH_3OH + F^-$ case, the abstracted hydrogen avoids the eclipsed conformation by only 10°. The transition state is of C_{2v} symmetry and has the long O−C internuclear separation of 1.916 Å. This bond is a bit shorter than the 2.000 Å bond length in the $[F\cdots CH3\cdots OH]^‡$ transition state but in qualitative features is very similar. In most cases, we observe excellent agreement among the present DFT and ab initio methods, particularly for the transition state. B3LYP predicts a C−O−H angle 4° larger than the ab initio methods. In addition, there are noticeable deviations between B3LYP and the ab initio methods for several dihedral angles. For torsional angles between the methyl hydrogens and the C−O−H plane, these deviations are usually about 10°. However, for τ(OHOH) and τ(COHO), these deviations are roughly 30°. We thus find DFT to deviate significantly from reliable ab initio values for parameters with flat surfaces, as is the case for many dihedral angles.

The structures associated with the identity reaction $CH_3SH + SH^-$ are very analogous to those seen in the OH case and are shown in Figure 6. We were unable to discover any prior

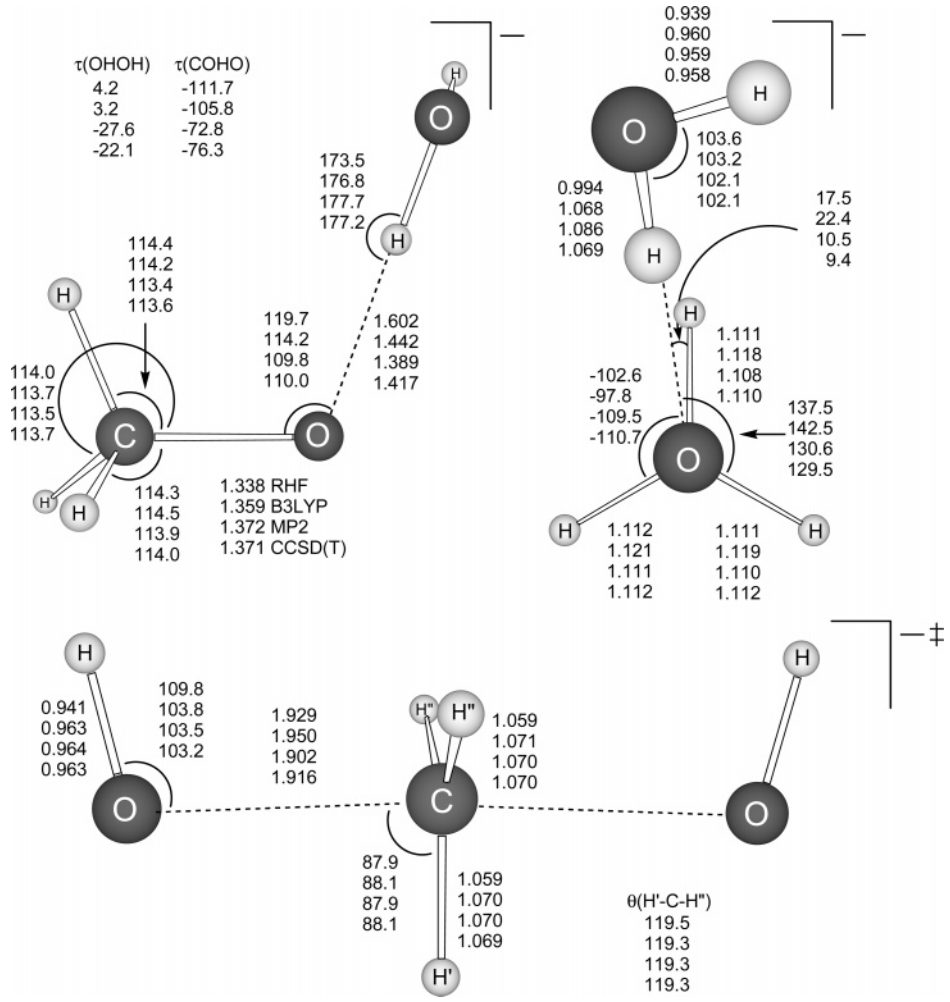

Figure 5. Geometries of the ion−molecule complex and transition state for the reaction $CH_3OH + OH^-$ using the TZ2Pf+dif basis set. All bond distances are in angstroms, and bond angles are in degrees. The ion−molecule complex is in C_1 symmetry, while the transition state is in C_{2v} symmetry. A Newman diagram is provided to clarify the orientations of the C_1 ion−molecule complex.

work on this reaction in the chemical literature. In the C_1 ion−molecule complex, the methoxy hydrogen is again almost eclipsing one of the methyl hydrogens, as compared with the anti nature of isolated CH_3SH. The methyl hydrogens H−C and H−C−S bond distances and bond angles are both a bit smaller than in the OH case. The key difference between this ion−molecule complex and the $CH_3OH\cdots OH^-$ complex is in the thiol hydrogens. In the OH case, the methoxy hydrogen had been essentially abstracted. That is not the case here; rather, the thiol S−H distance is only stretched about 0.06 Å with respect to isolated CH_3SH. The long S−H bond distance of 2.126 Å is also much larger than any of the long bonds in the OH case. The C_{2v} col is very similar to the OH transition state. The H−S−C angle is about 10° smaller than the H−O−C angle, and of course, the S−C distance is increased to 2.392 Å. Surprisingly, the agreement among DFT and the ab initio methods is better for this reaction than in the OH case. The only deviations of any note are small 5° deviations in the torsional angles involving the methyl hydrogens.

The stationary points associated with the $CH_3NH_2 + NH_2^-$ reaction are shown in Figure 7. Again, there is very little prior work on this identity exchange, limited to the prior work of Uggerud.[10] The ion−molecule complex is front side, with the nucleophile attracted to one of the acidic amine hydrogens. This connection is relatively short, 1.812 Å, but clearly, the amine hydrogen is not abstracted as was the case in the OH complex; the amine hydrogen attracted to the nucleophile has an N−H bond distance only 0.04 Å longer than the noninteracting N−H bond. The general structure of the CH_3NH_2 moiety is unchanged. The transition state, of C_{2v} symmetry, has the amine hydrogens pushed down just a bit from the unique methyl hydrogen. The long N−C bond length is about 2.01 Å. In gauging the performance of B3LYP with respect to the ab initio methods, we observe the same trends as for the OH identity reaction, namely, that all three methods are in excellent agreement for bond lengths and bond angles, but some large disparities exist in torsional angles, primarily for the ion−molecule complex. In particular, three torsional angles exhibit these large deviations, $\tau(N_5H_4N_2H_1)$, $\tau(H_6N_5H_4N_2)$, and $\tau(C_7H_5H_4N_2)$. Note that all of these are quantities mixed between the CH_3NH_2 and the NH_2^- moieties. This indicates that it is the relative placement of the NH_2^- moiety with which B3LYP is having some problems.

Finally, the last reaction considered is $CH_3PH_2 + PH_2^-$, shown in Figure 8. There is no prior work on this reaction, to our best knowledge. The nature of this reaction is similar to the previous reaction of $CH_3NH_2 + NH_2^-$. The reactant complex displays C_1 symmetry, with the nucleophile attracted to one of the acidic phosphine hydrogens. The placement of the PH_2^- moiety is different, however, as is evident in the different values of $\theta(X_5-H_4-X_2)$ (172.3° for NH_2 and 125.8° for PH_2) and $\tau(H_4-X_2-H_1-H_3)$ (−136.1° for NH_2 and 70.2° for PH_2). The structures of the isolated CH_3XH_2 and XH_2^- moieties are very similar as X changes from N to P. The distance between the two moieties is large, 3.101 Å, so one might expect the

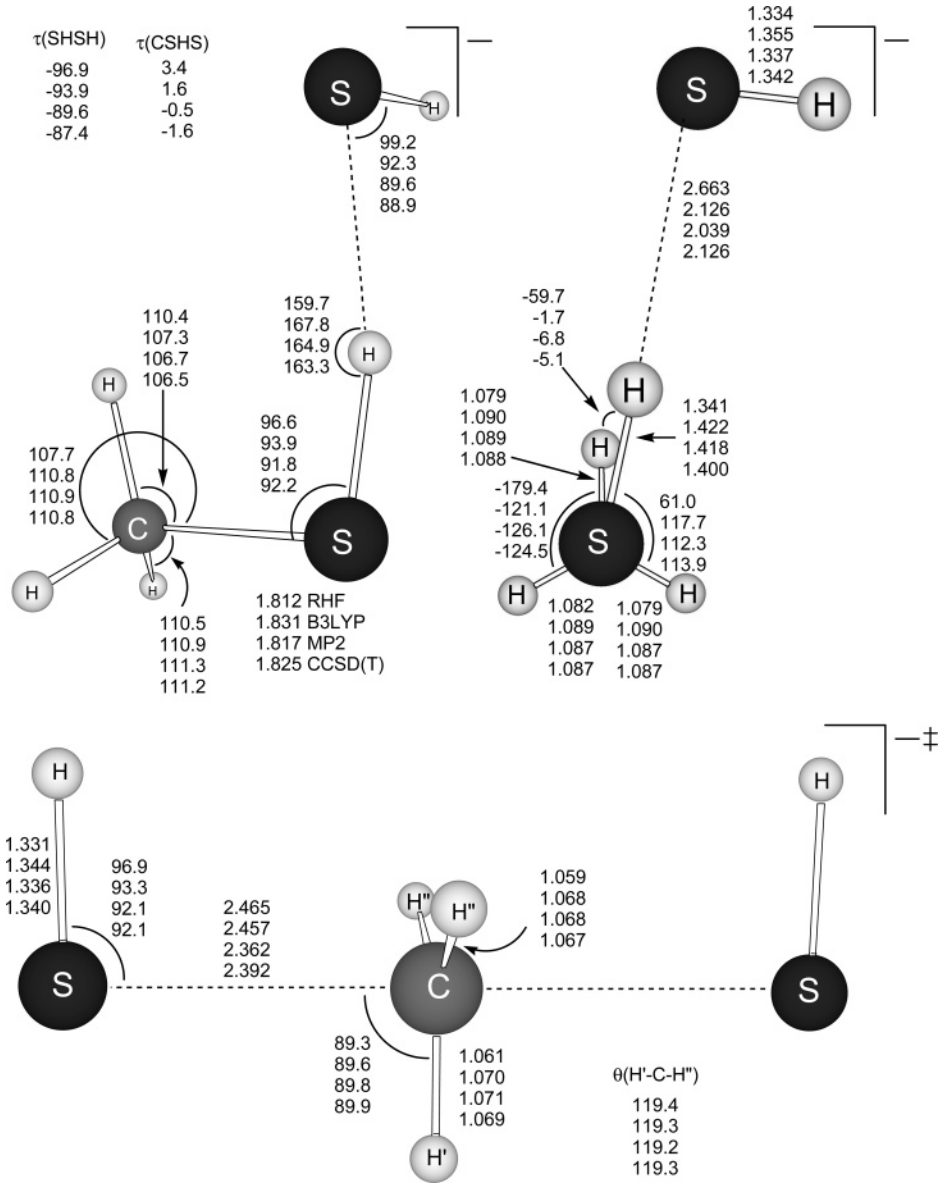

Figure 6. Geometries of the ion−molecule complex and transition state for the reaction $CH_3SH + SH^-$ using the TZ2Pf+dif basis set. All bond distances are in angstroms, and bond angles are in degrees. The ion−molecule complex is in C_1 symmetry, and the transition state is in C_{2v} symmetry. A Newman diagram is provided to clarify orientations of the C_1 ion−molecule complex.

interaction energy to be small. The transition state is structurally analogous to the amine case. Figure 8 reveals long C−P bonds of 2.5 Å and quasi-collinear heavy atoms. Interestingly, for this reaction, a second ion−molecule complex also exists, of the nature $CH_3PH^-\cdots PH_3$, shown in Figure 9. At the CCSD(T)/TZ2Pf+dif level, this structure lies 5.75 kcal mol^{-1} higher in energy than the previous complex. Essentially, PH_2^- has completely abstracted one of the acidic phosphine hydrogens. In all other respects, it is analogous to the $CH_3PH_2\cdots PH_2^-$ complex.

B. Complexation Energies (E^w). The complexation energy, E^w, defined in eq 3, measures the stabilization of the ion−molecule complex with respect to the reactants. Table 1 lists the complexation energies associated with the seven identity reactions computed with a combination of seven methods and three basis sets. The present discussion will be limited to the results utilizing the TZ2Pf+dif basis set, as basis set dependence is very small for the complexation energy. The focal point analysis of the seven reactions is included in Table 2. This includes all energetic quantities discussed in the methods section and shown in eq 6.

Before discussing individual reactions, general trends in the conventional and focal point data will be discussed. All of the complexation energies, save $E^w_{OH,OH}$, are less than 16 kcal mol^{-1}. In addition, there is general agreement among the methods; that is, CCSD(T) does not represent a drastic change over any of the other methods. This is consistent with our previous findings for complexation energies.[44,45] The focal point analyses are also in general agreement with the prior work. The increment $\delta(MP2^\infty)$ is almost always small with respect to the Hartree−Fock contribution, save in the thiol case. δ(CCSD) is almost always positive while δ[(T)] is always negative. Δ(ZPVE) and Δ(CC) are small but significant, and Δ(Rel) is always less than 0.035 kcal mol^{-1}.

It is also enlightening to examine individual reactions. The fluorine identity reaction has been discussed in detail before (see geometric structures section). We begin with an analysis of the chlorine reaction, which also has been the subject of very high level previous work, including the Weizmann extrapolations (including the effects of core correlation and scalar relativistic effects) performed by Parthiban, de Oliveira, and

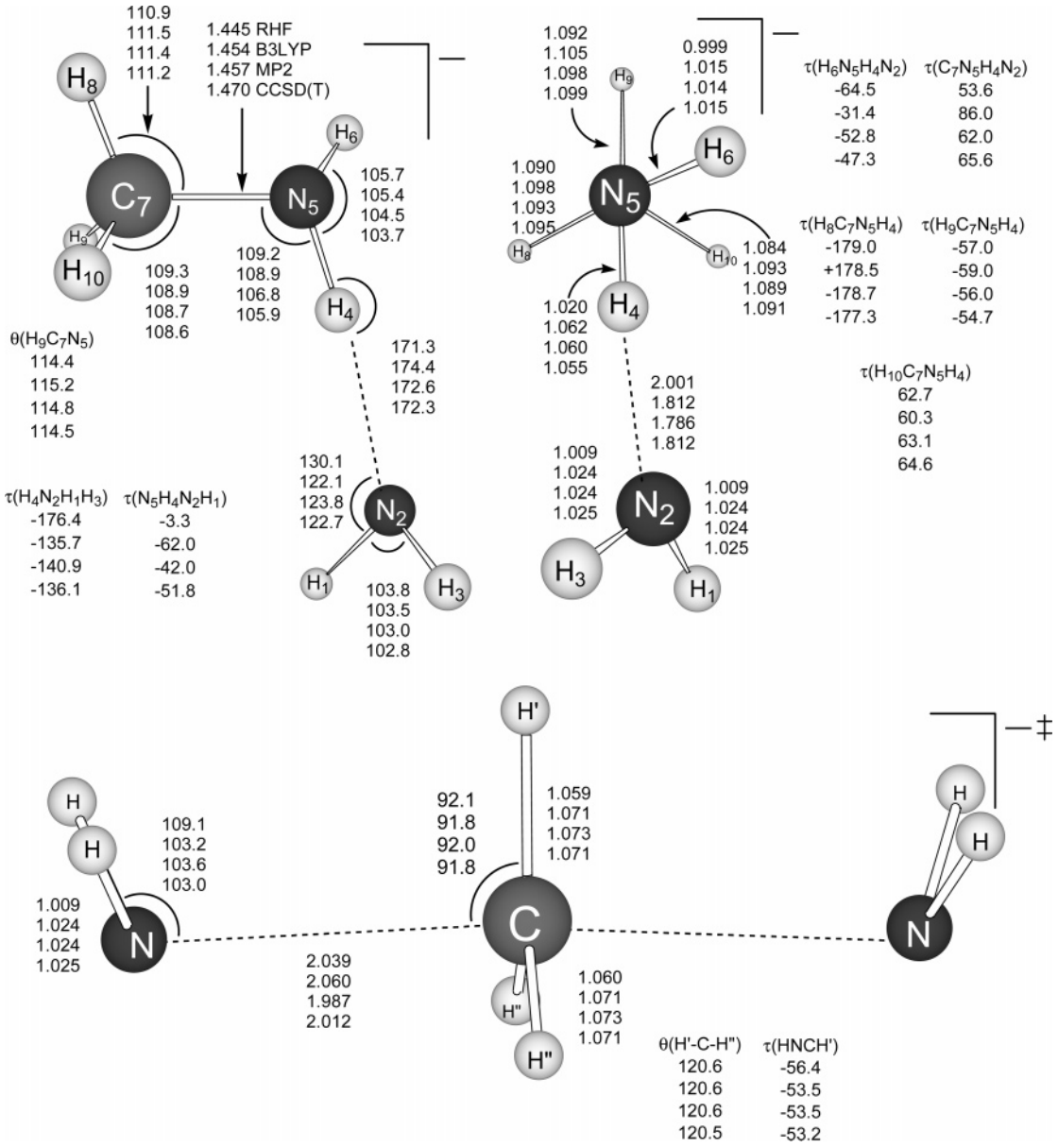

Figure 7. Geometries of the ion−molecule complex and transition state for the reaction $CH_3NH_2 + NH_2^-$ using the TZ2Pf+dif basis set for RHF, B3LYP, and MP2 and the TZ2P+dif basis set for CCSD(T). All bond distances are in angstroms, and bond angles are in degrees. The ion−molecule complex is in C_1 symmetry, while the transition state is in C_{2v} symmetry. A Newman diagram is provided to clarify the orientations of the C_1 ion−molecule complex.

Martin[42] and the QCISD(T) calculations of Lee et al.[43] The results in Table 1 indicate good agreement among the conventional methods, with an average complexation energy of about −10.5 kcal mol^{-1}. The focal point refinement obtains final values in good agreement with these and the high level prior works; including our zero-point correction in the Parthiban et al. result, the comparisons are Parthiban (−10.81), Lee(−10.63), present work (−11.03), and present work aug-cc-pV(X+d)Z series (−11.29).

For the cyano, and all subsequent, identity reactions, there are no previous results of acceptable quality. The earlier work of Uggerud[10] only considers complexes that follow classic backside form and thus are unusable in the present context. The conventional methods all compute a value for $E^{w}_{CN,CN}$ of approximately −12.5 kcal mol^{-1}, with CCSD(T)/TZ2Pf+dif being −12.44 kcal mol^{-1}. This is in excellent agreement with the focal point value of −12.60 kcal mol^{-1}.

The hydroxy identity reaction has a very large complexation energy, of over 30 kcal mol^{-1}. This can partially be explained in terms of the structure of the complex. In this complex, the acidic hydrogen has been abstracted by the nucleophile, forming a water molecule. The complex, which is essentially the water molecule loosely bound to the methoxy anion, is much more stable with respect to the reactants because the water O−H bond is stronger than the methanol O−H bond. CCSD(T)/TZ2Pf+dif predicts a value of −32.11 kcal mol^{-1}, within 1 kcal mol^{-1} of the final focal point value of −31.44 kcal mol^{-1}.

In contrast to the OH^- case, the complexation energy for SH^- is not large. Examination of the structures shows that the acidic hydrogen is not abstracted in this case; thus, the degree of stabilization is smaller. Note the distinction from the $CH_3XH_n\cdots F^-$ complex, in which the acidic hydrogen was abstracted only when X was a second-row atom. This ion−molecule complex has the largest deviation between the density functionals and the CCSD(T) reference. The difference between B3LYP and CCSD(T) (with the TZ2Pf+dif basis set) is 2.37 kcal mol^{-1}, while it is 1.6 kcal mol^{-1} for BLYP and 1.15 kcal mol^{-1} in the other direction for BP86. One possibility for this large deviation is a

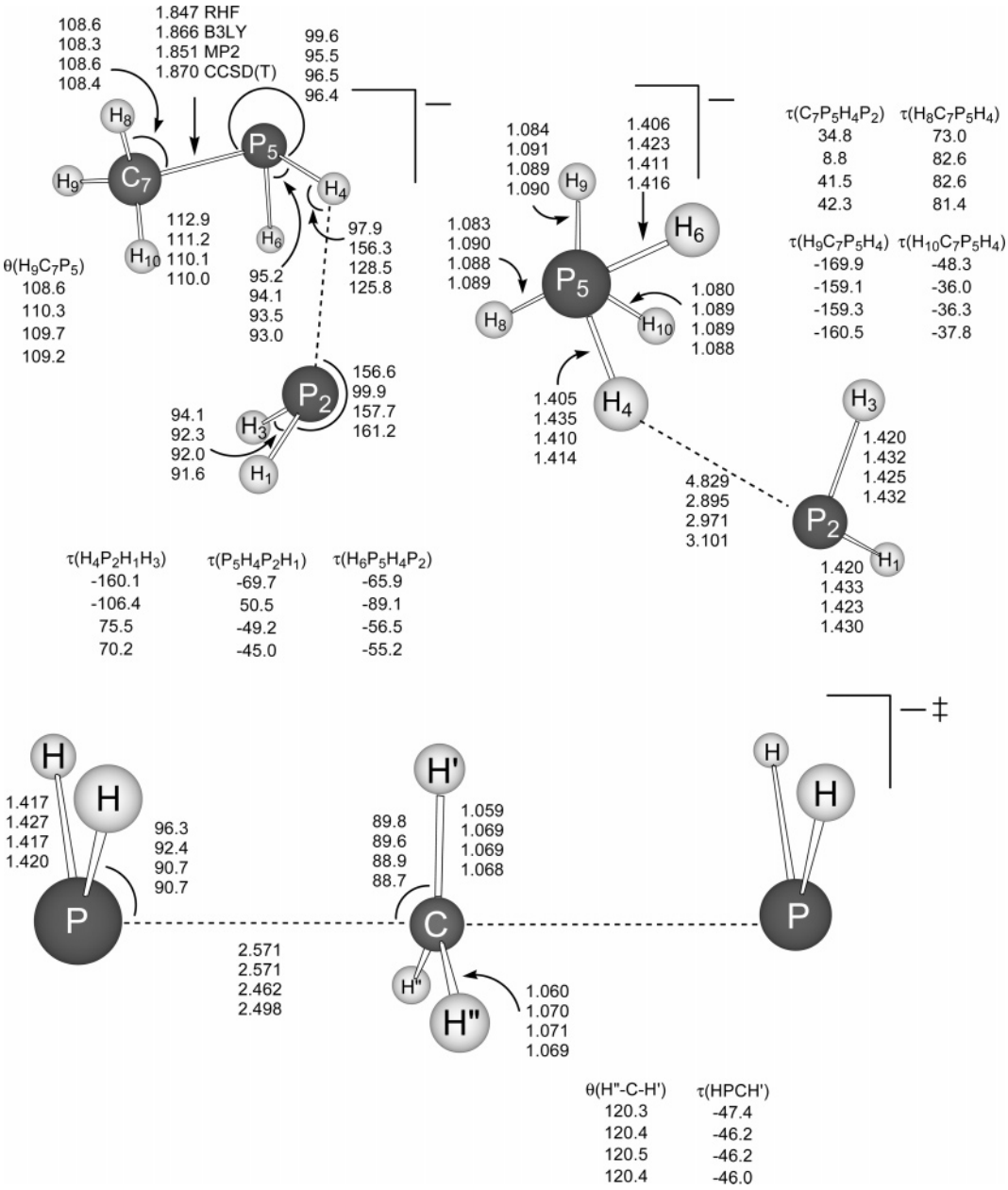

Figure 8. Geometries of the ion−molecule complex and transition state for the reaction $CH_3PH_2 + PH_2^-$ using the TZ2Pf+dif basis set for RHF, B3LYP, and MP2 and the TZ2P+dif basis set for CCSD(T). All bond distances are in angstroms, and bond angles are in degrees. The ion−molecule complex is in C_1 symmetry, while the transition state is in C_{2v} symmetry. A Newman diagram is provided to clarify the orientations of the C_1 ion−molecule complex.

possibility postulated by us in previous work, namely, that the TZ2Pf+dif basis set has deficiencies for sulfur. This is only partially supported by the focal point data, −12.86 and −12.92 kcal mol^{-1} (regular and +*d* series), both about 1 kcal mol^{-1} smaller in magnitude than the CCSD(T)/TZ2Pf+dif values.

The conventional methods compute values of $E^{w}_{NH_2,NH_2}$ of approximately −14 to −16 kcal mol^{-1}, with CCSD(T)/TZ2Pf+dif predicting a complexation energy of −15.63 kcal mol^{-1}. Agreement among the density functional and correlated methods is again excellent. The structure of the ion−molecule complex does not have any abstracted acidic hydrogens, and a value of −15.63 kcal mol^{-1} is consistent with this type of interaction. The final focal point value of −14.27 is surprisingly far removed (over 1.3 kcal mol^{-1}) from the TZ2Pf+dif values. Over half of this change is from the improved CCSD(T) description aug-cc-pVTZ provides over TZ2Pf+dif.

The $CH_3PH_2 + PH_2^-$ reaction has the smallest complexation energy, with a CCSD(T)/TZ2Pf+dif result of only −6.23 kcal mol^{-1}. This is a very small interaction energy, consistent with a primarily electrostatic interaction. Surprisingly, of the density functionals, B3LYP performs the poorest with respect to the CCSD(T) reference, underestimating the magnitude of the complexation energy by almost 2 kcal mol^{-1}. The final focal point energy of −5.63 (−5.66) decreases the magnitude of the interaction by 0.7 kcal mol^{-1}.

Table 3 lists some comparisons of several methods utilized in this paper. All of these values (save the final focal point energy) contain only electronic energies, i.e., no Δ(ZPVE), Δ(CC), or Δ(Rel). As such, one can compare accuracy across methods. As should be expected for the complexation energy, there is good agreement among all of the methods, with a few outliers. The outliers are for the most part due to deficiencies

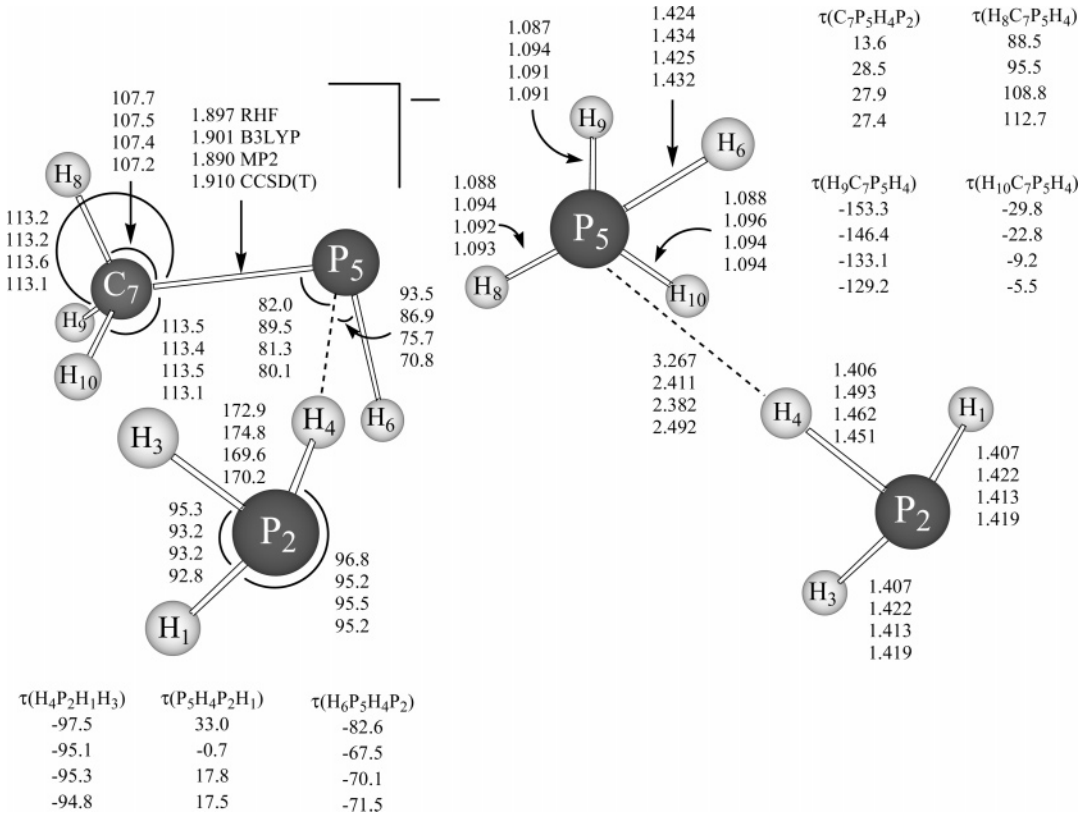

Figure 9. Geometries of the ion−molecule complex $CH_3PH^-\cdots PH_3$ using the TZ2Pf+dif basis set for RHF, B3LYP, and MP2 and the TZ2P+dif basis set for CCSD(T). All bond distances are in angstroms, and bond angles are in degrees. The ion−molecule complex is in C_1 symmetry. A Newman diagram is provided to clarify the orientations of the C_1 ion−molecule complex.

TABLE 1: Complexation Energies ($E^w_{X,X}$) Associated with the S_N2 Reactions (kcal mol^{-1})[a]

	RHF	B3LYP	BLYP	BP86	MP2	CCSD	CCSD(T)
				DZP+dif			
$E^w_{F,F}$	−12.35 (−12.03)	−13.02 (−12.87)	−13.06 (−13.02)	−12.88 (−12.88)	−13.07 (−12.84)	−13.20 (−12.98)	−13.42 (−13.19)
$E^w_{Cl,Cl}$	−9.15 (−8.95)	−9.72 (−9.71)	−9.87 (−9.97)	−10.05 (−10.11)	−9.91 (−9.80)	−9.78 (−9.67)	−10.01 (−9.89)
$E^w_{CN,CN}$	−11.20 (−10.70)	−13.12 (−12.66)	−13.12 (−12.74)	−13.86 (−13.57)	−12.84 (−12.37)	−12.30 (−11.83)	−12.67 (−12.20)
$E^w_{OH,OH}$	−25.31 (−24.61)	−32.11 (−32.58)	−31.59 (−32.27)	−33.88 (−34.65)	−31.33 (−31.70)	−30.94 (−31.31)	−31.83 (−32.20)
$E^w_{SH,SH}$	−7.85 (−7.07)	−12.35 (−11.93)	−12.88 (−12.65)	−15.42 (−15.43)	−12.85 (−12.41)	−11.48 (−11.04)	−12.33 (−11.89)
$E^w_{NH_2,NH_2}$	−12.80 (−11.41)	−16.09 (−15.17)	−16.00 (−15.23)	−17.22 (−16.80)	−17.00 (−15.90)	−16.17 (−15.07)	−16.95 (−15.85)
$E^w_{PH_2,PH_2}$	−3.80 (−3.32)	−5.11 (−4.66)	−5.69 (−5.33)	−7.11 (−6.92)	−6.10 (−5.36)	−5.45 (−4.70)	−6.09 (−5.34)
				TZ2P+dif			
$E^w_{F,F}$	−12.03 (−11.73)	−13.08 (−12.95)	−13.19 (−13.18)	−13.04 (−13.06)	−13.15 (−12.94)	−13.30 (−13.09)	−13.65 (−13.44)
$E^w_{Cl,Cl}$	−9.12 (−8.90)	−9.82 (−9.76)	−10.00 (−10.05)	−10.12 (−10.19)	−10.73 (−10.59)	−10.36 (−10.21)	−10.75 (−10.60)
$E^w_{CN,CN}$	−12.17 (−11.89)	−12.64 (−12.19)	−12.55 (−12.18)	−13.45 (−13.17)	−13.59 (−13.29)	−12.29 (−12.00)	−12.70 (−12.40)
$E^w_{OH,OH}$	−27.28 (−26.79)	−31.11 (−31.39)	−30.39 (−30.90)	−32.89 (−33.54)	−29.72 (−29.78)	−29.88 (−29.94)	−30.70 (−30.76)
$E^w_{SH,SH}$	−7.39 (−6.63)	−11.88 (−11.61)	−12.51 (−12.39)	−15.08 (−15.16)	−14.24 (−14.01)	−12.08 (−11.86)	−13.54 (−13.32)
$E^w_{NH_2,NH_2}$	−11.91 (−10.60)	−15.07 (−14.20)	−15.05 (−14.26)	−16.27 (−15.80)	−16.12 (−15.03)	−15.65 (−14.55)	−16.56 (−15.47)
$E^w_{PH_2,PH_2}$	−3.73 (−3.26)	−4.84 (−4.40)	−5.45 (−4.99)	−6.65 (−6.44)	−6.62 (−5.99)	−5.87 (−5.18)	−6.66 (−5.98)
				TZ2Pf+dif			
$E^w_{F,F}$	−11.85 (−11.54)	−12.87 (−12.74)	−12.93 (−12.91)	−12.79 (−12.81)	−12.91 (−12.71)	−13.14 (−12.93)	−13.49 (−13.28)
$E^w_{Cl,Cl}$	−8.86 (−8.65)	−9.57 (−9.51)	−9.70 (−9.75)	−9.85 (−9.91)	−10.62 (−10.49)	−10.22 (−10.09)	−10.70 (−10.57)
$E^w_{CN,CN}$	−12.14 (−11.86)	−12.65 (−12.20)	−12.57 (−12.20)	−13.48 (−13.20)	−12.90 (−12.47)	−12.43 (−12.00)	−12.88 (−12.44)
$E^w_{OH,OH}$	−27.69 (−27.23)	−31.43 (−31.75)	−30.71 (−31.25)	−33.19 (−33.85)	−31.00 (−31.33)	−30.80 (−31.13)	−31.78 (−32.11)
$E^w_{SH,SH}$	−7.31 (−6.57)	−11.78 (−11.50)	−12.40 (−12.27)	−14.96 (−15.02)	−14.87 (−14.63)	−12.41 (−12.17)	−14.10 (−13.87)
$E^w_{NH_2,NH_2}$	−11.89 (−10.59)	−15.07 (−14.23)	−15.06 (−14.30)	−16.29 (−15.86)	−16.35 (−15.39)	−15.61 (−14.65)	−16.59 (−15.63)
$E^w_{PH_2,PH_2}$	−3.76 (−3.29)	−4.78 (−4.42)	−5.39 (−4.89)	−6.57 (−6.36)	−6.88 (−6.29)	−5.95 (−5.36)	−6.83 (−6.23)

[a] The fluorine identity reaction results are taken from Gonzales et al.[44,45] The numbers in parentheses are zero-point corrected. CCSD and CCSD(T) energetics are zero-point corrected with MP2 frequencies.

in the TZ2Pf+dif basis set for second-row atoms. Note, in this regard, the B3LYP value for $E^w_{Cl,Cl}$ and the B3LYP, MP2, and CCSD(T)/TZ2Pf+dif values for $E^w_{SH,SH}$. These all have large deviations with respect to the CCSD(T)/aug-cc-pVTZ and extrapolated focal point valence limit. It must be emphasized that these "relatively" small deviations are still large on the scale

TABLE 2: Components of Extrapolated Complexation Energies, $E^w_{X,X}$ (kcal mol^{-1}), for S_N2 Reactions

	ΔE^{∞}_{RHF}	δ(MP2$^{\infty}$)	δ(CCSD)	δ[(T)]	Δ(ZPVE)	Δ(CC)	Δ(Rel)	final fp energy
$E^w_{F,F}$ [a]	−11.624	−1.669	−0.222	−0.444	0.205	0.020	0.008	−13.726
$E^w_{Cl,Cl}$	−8.475	−2.423	0.507	−0.471	0.129	−0.318	0.019	−11.033
$E^w_{Cl,Cl}$ (+d)[b]	−8.490	−2.679	0.526	−0.479	0.129	−0.318	0.019	−11.292
$E^w_{CN,CN}$	−10.392	−2.719	0.653	−0.498	0.432	−0.073	0.001	−12.596
$E^w_{OH,OH}$	−26.405	−3.973	0.109	−0.796	−0.328	−0.075	0.031	−31.436
$E^w_{SH,SH}$	−3.616	−10.481	2.838	−1.674	0.247	−0.203	0.031	−12.858
$E^w_{SH,SH}$ (+d)[b]	−3.682	−10.474	2.855	−1.690	0.247	−0.203	0.031	−12.916
$E^w_{NH_2,NH_2}$	−10.274	−4.774	0.767	−0.913	0.960	−0.035	0.002	−14.265
$E^w_{PH_2,PH_2}$	−1.465	−4.881	1.076	−0.890	0.209	0.278	0.042	−5.632
$E^w_{PH_2,PH_2}$ (+d)[b]	−1.490	−4.883	1.074	−0.891	0.209	0.278	0.042	−5.662

[a] The fluorine results are taken from the work of Gonzales et al.[45] [b] The suffix +d denotes that the aug-cc-pV(X+d)Z series was used for ΔE^{∞}_{RHF}, δ(MP2$^{\infty}$), δ(CCSD), and δ[(T)].

TABLE 3: Comparison of S_N2 Complexation Energies, $E^w_{X,X}$ (kcal mol^{-1}), Evaluated with Different Methods[a]

	B3LYP/ TZ2Pf+dif	MP2/ TZ2Pf+dif[c]	CCSD(T)/ TZ2Pf+dif[d]	CCSD(T)/ aug-cc-pVTZ[c]	extrapolated fp valence limit[e]	final fp energy[f]
$E^w_{F,F}$ [b]	−12.87	−12.92	−13.49	−14.15	−13.96	−13.73
$E^w_{Cl,Cl}$	−9.57	−10.62	−10.70	−10.89 (−10.81)[g]	−10.86 (−11.12)	−11.03 (−11.29)
$E^w_{CN,CN}$	−12.65	−12.90	−12.88	−13.18	−12.96	−12.60
$E^w_{OH,OH}$	−31.43	−31.00	−31.78	−31.50	−31.06	−31.44
$E^w_{SH,SH}$	−11.78	−14.87	−14.10	−13.32 (−13.02)	−12.93 (−12.99)	−12.86 (−12.92)
$E^w_{NH_2,NH_2}$	−15.07	−16.35	−16.59	−15.85	−15.19	−14.27
$E^w_{PH_2,PH_2}$	−4.78	−6.88	−6.83	−6.60 (−6.47)	−6.16 (−6.19)	−5.63 (−5.66)

[a] Only the final focal point energy includes the zero-point correction. [b] The fluorine values are taken from Gonzales et al.[44,45] [c] Core electrons are frozen. [d] Core electrons are not frozen. [e] Extrapolated focal point (fp) limit without Δ(ZPVE), Δ(CC), and Δ(Rel). [f] Extrapolated focal point (fp) limit with Δ(ZPVE), Δ(CC), and Δ(Rel). [g] Quantities in parentheses are evaluated or extrapolated with the aug-cc-pV(X+d)Z series.

of chemical accuracy. Finally, the effect of the tight d function is small but not negligible. The magnitudes of the deviations were 0.26, 0.06, and 0.03 kcal mol^{-1} for $E^w_{Cl,Cl}$, $E^w_{SH,SH}$, and $E^w_{PH_2,PH_2}$, respectively.

C. Net and Central Activation Barriers (E^b and E^*). The net activation barrier, defined in eq 4, represents the relative height of the transition state with respect to the reactants. A negative number indicates that the transition state lies below the reactants, while a positive number indicates that the transition state lies higher in energy. Table 4 lists the conventional net activation barriers associated with the seven methods utilized. Table 5 presents the focal point analyses of said reactions. Before considering individual reactions, a few general comments are warranted. In contrast to the E^w computations, here, we observe significant basis set dependence for the correlated methods, particularly in increasing the basis set size from DZP+dif to TZ2P+dif. As has been observed before,[44] DFT performs poorly in this respect, particularly the pure functionals, underestimating the size of the barrier by 3−7 kcal mol^{-1}. In addition, all of the barriers, save the fluorine case, have positive magnitudes, with five having barriers greater than 13 kcal mol^{-1}. The focal point predictions include much larger δ(MP2$^{\infty}$) values (again as observed before for the E^b values[45]). δ(CCSD) and δ[(T)] are also larger in magnitude than was observed for E^w. In particular, δ[(T)] is often on the order of 3 kcal mol^{-1} indicating possible diradical character in the transition state. The T1 and T2 amplitudes were examined to confirm single reference character of the correlated wave functions. Clearly, to adequately describe these species, triple excitations are absolutely critical. Finally, Δ(CC) and Δ(Rel) are now significant (on the chemical accuracy scale), with values often greater than 0.1 kcal mol^{-1}.

As mentioned earlier, the chlorine identity reaction has been heavily studied. In addition to the prior high level works of Parthiban et al. and Lee et al., Botschwina has utilized CCSD(T) in conjunction with basis sets of up to aug-cc-pV5Z quality. The agreement between these high level works and the present one is good: Parthiban (2.38), Lee (3.00), Botschwina (2.27), and present work (1.85), the latter with the aug-cc-pV(X+d)Z basis sets (1.57). The large magnitude of the Lee result is disturbing and is partially due to the limited use of higher angular momentum functions; that is, their basis set is 6-311++G(3df,2p). This compares with all of the other calculations that include up to h functions. Also important to remember is the fact that all of these computations utilize different reference geometries.

The next barrier to consider is for the $CH_3CN + CN^-$ reaction. This is a very large barrier of over 28 kcal mol^{-1}. The density functionals again spuriously stabilize the transition state, leading to smaller barriers. The final focal point net activation barrier of 28.69 kcal mol^{-1} is the largest computed in this study and is surpassed only by E^b_{F,NH_2} in the previous study.[45]

Because the OH and SH transition states have similar structural features, one might expect them both to have similar net activation barriers. This is indeed the case with both barriers hovering about 14 kcal mol^{-1}; the conventional CCSD(T)/TZ2P+dif results are 13.77 and 13.15 kcal mol^{-1}, respectively, for $E^b_{OH,OH}$ and $E^b_{SH,SH}$. The focal point results are about 0.6 kcal mol^{-1} larger, with the OH barrier at 14.30 kcal mol^{-1}, while the SH focal point barriers are 13.86 and 13.76 kcal mol^{-1}. Note the large magnitude of Δ[(T)] for OH and SH, again emphasizing the importance of correlation beyond CCSD to accurately describe the barrier energetics of these systems. Even

TABLE 4: Net Activation Energies ($E^{b}_{X,X}$) associated with the S_N2 Reactions (kcal mol^{-1})[a]

	RHF	B3LYP	BLYP	BP86	MP2	CCSD	CCSD(T)
				DZP+dif			
$E^{b}_{F,F}$	8.14 (7.95)	−2.09 (−2.42)	−5.90 (−6.34)	−5.27 (−5.71)	1.82 (1.54)	3.10 (2.82)	1.16 (0.88)
$E^{b}_{Cl,Cl}$	6.59 (6.09)	−0.76 (−1.31)	−4.36 (−4.99)	−3.93 (−4.50)	8.15 (7.55)	7.73 (7.13)	5.93 (5.33)
$E^{b}_{CN,CN}$	35.68 (35.50)	26.83 (26.43)	23.02 (22.46)	23.32 (22.76)	32.42 (31.74)	32.62 (31.94)	30.04 (29.36)
$E^{b}_{OH,OH}$	27.23 (27.06)	13.35 (12.93)	8.13 (7.43)	8.91 (8.26)	16.55 (16.06)	18.95 (18.45)	16.11 (15.62)
$E^{b}_{SH,SH}$	23.87 (23.37)	11.10 (10.44)	6.27 (5.54)	6.43 (5.80)	19.87 (19.08)	3.60 (2.82)	−0.66 (−1.45)
$E^{b}_{NH_2,NH_2}$	43.66 (43.29)	26.87 (26.36)	20.78 (19.98)	21.45 (20.80)	30.45 (29.81)	33.48 (32.83)	29.91 (29.26)
$E^{b}_{PH_2,PH_2}$	40.67 (40.10)	22.10 (21.43)	16.25 (15.42)	15.99 (15.25)	30.86 (29.20)	32.34 (30.67)	28.72 (27.05)
				TZ2P+dif			
$E^{b}_{F,F}$	6.95 (6.91)	−3.72 (−3.92)	−7.44 (−7.76)	−6.89 (−7.20)	−1.00 (−1.03)	0.33 (0.30)	−2.15 (2.18)
$E^{b}_{Cl,Cl}$	5.92 (5.60)	−1.65 (−2.07)	−5.06 (−5.57)	−4.44 (−4.93)	2.25 (2.11)	3.26 (3.12)	1.23 (1.08)
$E^{b}_{CN,CN}$	35.82 (35.72)	27.86 (27.53)	24.17 (23.67)	24.35 (23.85)	30.12 (29.96)	30.30 (30.14)	27.52 (27.37)
$E^{b}_{OH,OH}$	25.80 (25.82)	11.82 (11.60)	6.71 (6.26)	7.37 (7.01)	13.28 (13.23)	15.88 (15.83)	12.42 (12.37)
$E^{b}_{SH,SH}$	23.33 (22.93)	10.24 (9.71)	5.49 (4.88)	5.92 (5.40)	13.61 (13.32)	15.85 (15.56)	12.61 (12.32)
$E^{b}_{NH_2,NH_2}$	42.99 (42.67)	26.04 (25.58)	19.86 (19.16)	20.53 (19.96)	27.16 (26.81)	30.51 (30.16)	26.37 (26.01)
$E^{b}_{PH_2,PH_2}$	40.44 (39.87)	21.39 (20.76)	15.52 (14.77)	15.53 (14.85)	24.79 (24.13)	28.02 (27.36)	23.79 (23.13)
				TZ2Pf+dif			
$E^{b}_{F,F}$	8.14 (8.05)	−2.81 (−3.05)	−6.62 (−6.97)	−6.05 (−6.39)	0.69 (0.53)	2.15 (1.99)	−0.38 (−0.53)
$E^{b}_{Cl,Cl}$	7.20 (6.87)	−0.76 (−1.17)	−4.29 (−4.79)	−3.66 (−4.14)	3.65 (3.36)	4.89 (4.59)	2.57 (2.28)
$E^{b}_{CN,CN}$	36.44 (36.33)	28.35 (28.01)	24.62 (24.11)	24.78 (24.27)	31.46 (31.21)	32.03 (31.78)	29.21 (28.95)
$E^{b}_{OH,OH}$	26.66 (26.67)	12.45 (12.23)	7.29 (6.84)	7.94 (7.58)	14.59 (14.47)	17.42 (17.30)	13.89 (13.77)
$E^{b}_{SH,SH}$	24.32 (23.92)	10.90 (10.39)	6.08 (5.49)	6.45 (5.96)	14.31 (13.91)	17.10 (16.70)	13.55 (13.15)
$E^{b}_{NH_2,NH_2}$	43.52 (43.19)	26.43 (25.99)	20.22 (19.54)	20.85 (20.29)	27.98 (27.54)	31.74 (31.30)	27.49 (27.05)
$E^{b}_{PH_2,PH_2}$	41.15 (40.59)	21.83 (21.23)	15.92 (15.21)	15.83 (15.20)	25.05 (24.37)	29.14 (28.45)	24.64 (23.95)

[a] The fluorine identity reaction results are taken from Gonzales et al.[44,45] The numbers in parentheses are zero-point corrected. CCSD and CCSD(T) energetics are zero-point corrected with MP2 frequencies.

TABLE 5: Components of Extrapolated Net S_N2 Activation Barriers, $E^{b}_{X,X}$ (kcal mol^{-1})

	ΔE^{∞}_{RHF}	δ(MP2$^{\infty}$)	δ(CCSD)	δ[(T)]	Δ(ZPVE)	Δ(CC)	Δ(Rel)	final fp energy
$E^{b}_{F,F}$ [a]	8.459	−8.019	1.351	−2.627	−0.159	0.245	−0.054	−0.805
$E^{b}_{Cl,Cl}$	8.735	−4.969	0.975	−2.398	−0.292	−0.110	−0.093	1.848
$E^{b}_{Cl,Cl}$ (+d)[b]	8.668	−5.235	1.059	−2.427	−0.292	−0.110	−0.093	1.570
$E^{b}_{CN,CN}$	36.999	−5.706	0.178	−2.928	−0.251	0.479	−0.079	28.692
$E^{b}_{OH,OH}$	27.484	−12.409	2.662	−3.534	−0.121	0.318	−0.096	14.304
$E^{b}_{SH,SH}$	25.967	−10.707	2.604	−3.528	−0.399	0.055	−0.132	13.860
$E^{b}_{SH,SH}$ (+d)[b]	25.807	−10.673	2.675	−3.571	−0.399	0.055	−0.132	13.762
$E^{b}_{NH_2,NH_2}$	44.939	−15.946	3.548	−4.249	−0.440	0.406	−0.102	28.605
$E^{b}_{PH_2,PH_2}$	43.014	−16.970	4.371	−4.573	−0.638	0.353	−0.144	25.413
$E^{b}_{PH_2,PH_2}$ (+d)[b]	42.930	−16.951	4.663	−4.502	−0.638	0.353	−0.144	25.711

[a] The fluorine values are taken from Gonzales et al.[45] [b] The suffix +d denotes that the aug-cc-pV(X+d)Z series was used for ΔE^{∞}_{RHF}, δ(MP2$^{\infty}$), δ(CCSD), and δ[(T)].

the focal point analyses indicate comparable values for the various incremental and nonincremental terms. The change between the conventional and +d basis sets is very small for $E^{b}_{SH,SH}$.

The barrier heights for the NH_2 and PH_2 reactions are strikingly similar. The CCSD(T)/TZ2Pf+dif results are 27.05 kcal mol^{-1} for NH_2 and 23.95 kcal mol^{-1} for PH_2. Both have the interesting characteristic that the (T) contribution is very large, lowering the barrier by 4 kcal mol^{-1} in both cases. The final focal point barriers are 28.605 and 25.413 (25.711) kcal mol^{-1} for NH_2 and PH_2 [PH_2(+d)], respectively. As in the OH and SH cases, the magnitude of Δ[(T)] is very large, in fact the largest of any series of reactions studied in this or previous work. Clearly, the (T) contribution is important in correctly describing these energetics. The focal point procedure increases the barrier heights in both cases by 1.5 kcal mol^{-1}, more strong evidence supporting the necessity of energy refinement if chemical accuracy is required.

Finally, Table 6 lists some comparisons among the various methods utilized in this paper. Clearly, the density functional values are performing poorly, with barrier deviations of about 3 kcal mol^{-1} with the correlated results. MP2 does poorly as well. Even CCSD can have major deficiencies; only when one includes a perturbative correction for connected triples [δ[(T)]] do energetics converge to within chemical accuracy. Still the variation between the TZ2Pf+dif and aug-cc-pVXZ results is significant, over 1 kcal mol^{-1} for CN. The difference between the extrapolated values and the CCSD(T)/aug-cc-pVTZ results clearly indicates that the focal point (or like-minded) technique is necessary to obtain chemical (or subchemical) accuracy. For E^{w}, the effect of the tight d function was small, but it is very significant in this case. The barriers magnitudes are increased in all cases, by 0.43, 0.50, and 0.51 kcal mol^{-1} for the cases of

TABLE 6: Comparison of Net Barriers, $E^b_{X,X}$ (kcal mol^{-1}), Evaluated with Different Methods[a]

	B3LYP/ TZ2Pf+dif	MP2/ TZ2Pf+dif[c]	CCSD(T)/ TZ2Pf+dif[d]	CCSD(T)/ aug-cc-pVTZ[c]	extrapolated fp valence limit[e]	final fp energy[f]
$E^b_{F,F}$[b]	−2.81	0.69	−0.38	−1.11	−0.84	−0.81
$E^b_{Cl,Cl}$	−0.76	3.65	2.57	1.64 (2.07)[g]	2.34 (2.07)	1.85 (1.57)
$E^b_{CN,CN}$	28.35	31.46	29.21	27.97	28.54	28.69
$E^b_{OH,OH}$	12.45	14.59	13.89	13.46	14.20	14.30
$E^b_{SH,SH}$	10.90	14.31	13.55	13.15 (13.65)	14.34 (14.24)	13.86 (13.76)
$E^b_{NH_2,NH_2}$	26.43	27.98	27.49	27.40	28.74	28.61
$E^b_{PH_2,PH_2}$	21.83	25.05	24.64	24.33 (24.84)	25.84 (26.14)	25.41 (25.71)

[a] Only the final focal point energy includes the zero-point correction. [b] The fluorine identity values are taken from Gonzales et al.[44,45] [c] Core electrons are frozen. [d] Core electrons are not frozen. [e] Extrapolated focal point (fp) limit without Δ(ZPVE), Δ(CC), and Δ(Rel). [f] Extrapolated focal point (fp) limit with Δ(ZPVE), Δ(CC), and Δ(Rel). [g] Quantities in parentheses are evaluated or extrapolated with the aug-cc-pV(X+d)Z series.

TABLE 7: CCSD(T)/TZ2Pf+dif Central Barriers, $E^*_{X,Y}$, Associated with Nonidentity Reactions of the Type CH_3X + F^- (kcal mol^{-1})[a]

	explicit	explicit-collinear[b]	Marcus	Marcus-collinear[c]
$E^*_{F,Cl}$	3.70		3.82	
$E^*_{Cl,F}$	28.07		28.19	
$E^*_{F,CN}$	38.49	33.06	37.18	34.09
$E^*_{CN,F}$	20.76		19.45	
$E^*_{F,OH}$	47.84	26.38	50.87	37.73
$E^*_{OH,F}$	10.73		13.77	
$E^*_{F,SH}$	41.99	15.29	32.35	17.73
$E^*_{SH,F}$	20.80		11.16	
E^*_{F,NH_2}	55.01	24.51	56.46	47.42
$E^*_{NH_2,F}$	8.67		10.12	
E^*_{F,PH_2}[d]	43.02	30.60	37.59	39.96
$E^*_{PH_2,F}$	16.40		10.97	

[a] (F,X) values are forward barriers while (X,F) is meant to describe the reverse barriers. [b] Collinear indicates that the ion−molecule complex used to compute the barrier has constrained collinear heavy atoms. [c] Collinear indicates that the Marcus barriers were evaluated using the collinear structures for energy references. [d] The PH_2 values are CCSD(T)/TZ2P+dif.

Cl, SH, and PH_2, respectively. Clearly, this is significant when chemical accuracy is desired.

D. Marcus Theory. As discussed in the Introduction, Marcus theory allows one to compute the central activation barrier of the reaction $CH_3X + Y^-$, E^* (eq 5), as a function of two quantities: the thermodynamic driving force, E^0, and the intrinsic barrier, E^*_0. E^*_0 can be approximated from the intrinsic barriers of the associated identity reactions $CH_3X + X^-$ and $CH_3Y + Y^-$, as in eq 2. We have performed the Marcus analysis on 12 central barriers associated with reactions of the type $CH_3X + F^-$ and $CH_3F + X^-$ with X = Cl, CN, OH, SH, NH_2, and PH_2. Recall that in prior work we computed explicit values for these barriers, which can be compared with values computed here. Finally, because some of the S_N2 reactions do not have classic backside structures, we also explicitly computed the barriers using constrained collinear structures (i.e., all three heavy atoms constrained to be collinear) as a reference. Additionally, we have used these constrained structures for additional Marcus theory calculations. The geometries and energetics of these species will not be discussed here, but B3LYP, MP2, and CCSD(T)/TZ2Pf+dif optimized geometries and energies can be found in the Supporting Information.

Table 7 lists the various techniques for obtaining the central barriers, while Chart 1 illustrates the data in graphical form.

CHART 1: Plot of Marcus Theory vs Explicit Central Barriers (Data Taken from Table 7)[a]

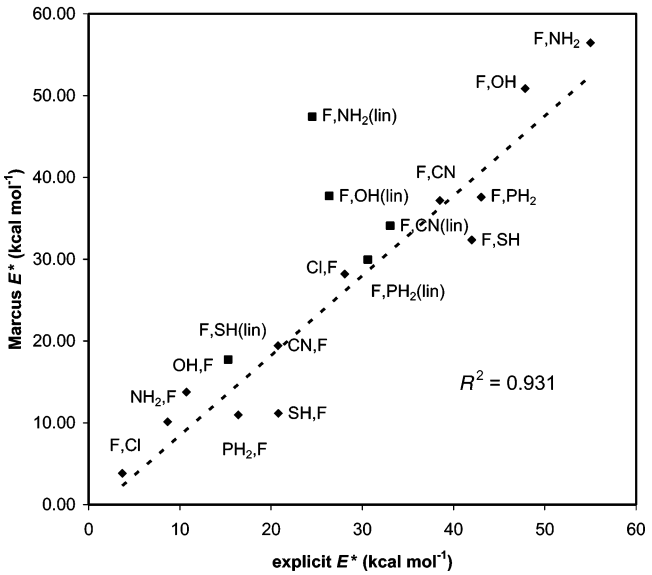

[a] The points include both the conventional (diamonds) and the explicit values (squares). A least squares fit of the conventional data is shown to have some linear character, but clearly, the outliers detract from the linear correlation.

Focusing on the Marcus data, one can see that explicit calculations and Marcus theory are in excellent agreement for the first two central barriers, namely, those associated with the classic $CH_3Cl + F^-$ reaction. The rest of the data shows some sizable deviations. Let us focus on the Marcus column first. Not including the chlorine data, the smallest deviation between Marcus theory and explicit computation is 1.31 for both cyano barriers. In many cases, the deviation is much worse. In particular, the PH_2 and SH barriers deviate by 6 and 9 kcal mol^{-1}, respectively. The constrained collinear structures also exhibit sizable deviations, including a deviation of over 22 kcal mol^{-1} for E^*_{F,NH_2}.

One can ask the question, is it possible to compute Marcus theory values that are independent of the well depths associated with the ion−molecule complexes? The answer is yes, and several groups have augmented the original Marcus theory to evaluate E^b, a quantity independent of the well depths. Wolfe,

TABLE 8: CCSD(T)/TZ2Pf+dif Net Activation Barriers, $E^{b}_{X,Y}$, Associated with Nonidentity Reactions of the Type $CH_3X + F^-$ (kcal mol^{-1})[a]

	explicit	augmented Marcus
$E^{b}_{F,Cl}$	−11.28	−9.54
$E^{b}_{Cl,F}$	18.24	19.98
$E^{b}_{F,CN}$	14.68	15.75
$E^{b}_{CN,F}$	12.04	13.11
$E^{b}_{F,OH}$	17.76	18.08
$E^{b}_{OH,F}$	−3.05	−2.72
$E^{b}_{F,SH}$	4.70	3.46
$E^{b}_{SH,F}$	11.21	9.98
E^{b}_{F,NH_2}	36.04	37.20
$E^{b}_{NH_2,F}$	−4.18	−3.02
E^{b}_{F,PH_2}	22.86	20.34
$E^{b}_{PH_2,F}$	7.72	5.20

[a] (F,X) values are forward barriers while (X,F) describes the reverse barriers. The augmented Marcus theory values were obtained using eq 7.

CHART 2: Plot of Marcus Theory vs Explicit Net Activation Barriers (Data Taken from Table 8)[a]

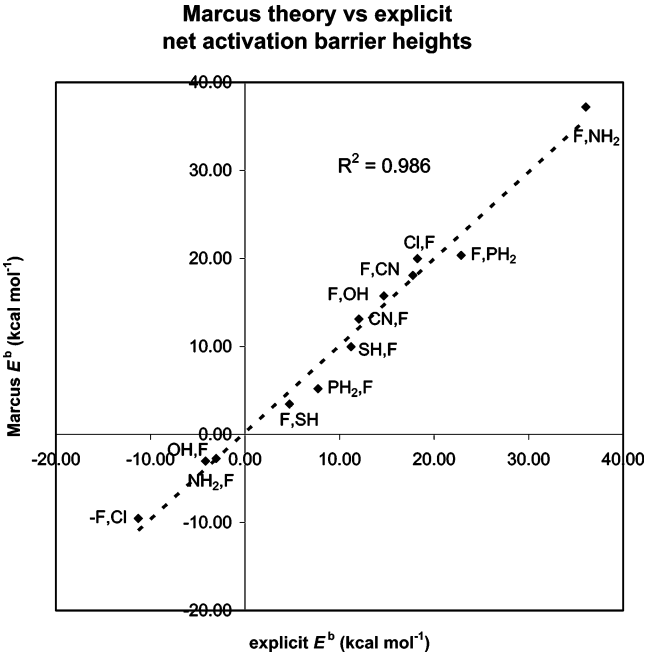

[a] Note the linear spread of data with a correlation coefficient of 0.986.

Mitchell, and Schlegel,[58] in addition to Dodd and Brauman,[26] have proposed using the following form for E^{b}.

$$E^{b} = E^{b}_{0} + \frac{E^{0}}{2} + \frac{(E^{0})^{2}}{8(E^{*}_{X,X} + E^{*}_{Y,Y})} \qquad (7)$$

This form is completely independent of the well depths and thus may be free of some of the problems that we experienced with E^{*}.

Table 8 lists the ab initio and augmented Marcus results for E^{b}, and Chart 2 plots the same data. There is much less variability among these data, with the largest deviation being 2.52 kcal mol^{-1} for the PH_2 barriers. The plot in Chart 2 shows a linear spread of data with a correlation coefficient of 0.986. Clearly, the performance of "Marcus" theory for these quantities is superior to what was achieved for E^{*}. In this context, the important reaction dynamics studies of Hase[128] demonstrate that the deep attractive well in S_N2 reactions may be "flown over" in trajectory studies. Hase has also shown[129,130] that the well depth is irrelevant in computing rate constants, as long as transition state recrossing is not important.

Summary

A comprehensive database of gas phase S_N2 reactions of the type $CH_3X + F^-$ (X = F, Cl, CN, OH, SH, NH_2, PH_2) has been combined with results for the $CH_3X + X^-$ reaction (X = F, Cl, CN, OH, SH, NH_2, PH_2). Optimized geometries for all stationary points are available with any combination of seven methods [RHF, B3LYP, BLYP, BP86, MP2, CCSD, and CCSD(T)] and three basis sets (DZP+dif, TZ2P+dif, and TZ2Pf+dif). Harmonic vibrational frequencies are available for all of the above, save CCSD and CCSD(T). Additionally, the focal point procedure, utilizing basis sets of up to aug-cc-pV5Z quality, in conjunction with correlation treatments up to CCSD(T), was used to definitively assign values for all energetic quantities (E^{w}, E^{b}, E^{*}, and E^{0}) to within 1 kcal mol^{-1}. The effects of core correlation and relativity were also evaluated and included in final energetic predictions. The complete data set is available in the Supporting Information of this paper.

When specifically considering the identity reactions detailed in the present paper, a wide range of energetic and structural features are manifested. The range of complexation energies is −5.66 to −31.44 kcal mol^{-1}, while for net activation barriers the range is −0.81 to 28.69 kcal mol^{-1}. The nature of the complexes varies significantly with X. For X = F, Cl, the complexes are classic backside complexes with all heavy atoms collinear. The complex associated with X = CN is backside but not collinear. The rest of the complexes (X = OH, SH, NH_2, and PH_2) are frontside complexes with the nucleophile attracted to an acidic hydrogen. The OH complex is unique, as the OH^- nucleophile abstracts the acidic methanol hydrogen, forming a very strong water O−H bond. This results in a very large complexation energy, over 16 kcal mol^{-1} relatively more stable than any other complex. None of the other frontside complexes abstracts an acidic hydrogen. All of the transition states exhibit the same qualitative character, with quasi-linear heavy atoms and symmetry of at least C_{2v} and, in three cases, D_{3h} (X = F, Cl, CN).

The components of the focal point energy analysis also exhibit several interesting trends, as highlighted in Table 9. In both cases, the δ(MP2$^{\infty}$) contribution is large, but for E^{b}, the magnitude is huge, averaging over 10 and reaching as large as 17 kcal mol^{-1}. In all cases, for both E^{w} and E^{b}, this lowers the energy, stabilizing the complex and transition state with respect

TABLE 9: Statistics for Increments (kcal mol^{-1}) to S_N2 Energetics[a]

	δ(MP2$^{\infty}$)	δ(CCSD)	δ[(T)]	Δ(CC)	Δ(Rel)
E^{w}	4.45 (100, 10.48)	0.88 (14, 2.86)	0.82 (100, 1.69)	0.14 (71, 0.32)	0.02 (0, 0.42)
E^{b}	10.71 (100,16.95)	2.31 (0, 4.66)	3.41 (100, 4.50)	0.28 (14. 0.48)	0.10 (100, 0.14)

[a] δ increments refer to changes with respect to the previous level of theory, MP2 change from HF, CCSD from MP2, and CCSD(T) from CCSD. Δ increments are absolute magnitude changes (see Computational Methods section of text for details). The principal entries are mean absolute values. The numbers in parentheses are the percentages of the increments that decrease the relative energy followed by the maximum absolute deviations.

to the reactants. As should be expected, the value of δ(CCSD) is small for E^w and larger for E^w. What is most striking is the magnitude of δ[(T)], over 3.4 kcal mol^{-1}. This indicates that correlation levels up to CCSD(T) are critical in describing the energetics of these systems to within 1 kcal mol^{-1}. The effects of quadruple and higher excitations are less than 0.5 kcal mol^{-1} in all but the most extreme cases. The magnitude of the auxiliary correlations for core correlation [Δ(CC)] and relativistic effects [Δ(Rel)] never exceeds 0.32 kcal mol^{-1}, small but still significant when chemical accuracy is desired. As mentioned in the theoretical methods, using MP2 instead of CCSD(T) for core correlation probably increases our error bars by 0.1−0.2 kcal mol^{-1} but still maintains chemical accuracy.

An important issue to consider is the nature of the basis set convergence, specifically what type of improvement is achieved in the progression from CCSD(T)/TZ2Pf+dif to CCSD(T)/aug-cc-pVTZ to the focal point limit. To do this, we compute the (average, maximum) deviation with respect to the focal point limit for CCSD(T)/TZ2Pf+dif and CCSD(T)/aug-cc-pVTZ. For E^w, the results are (0.69, 1.40) and (0.30, 0.66), respectively (all units in kcal mol^{-1}). For E^b, the results are (0.77, 1.50) and (0.69, 1.34). This clearly indicates that neither CCSD(T)/TZ2Pf+dif nor CCSD(T)/aug-cc-pVTZ solely are adequate in describing these energetics to within 1 kcal mol^{-1}. The inclusion of a set of tight *d* function for second-row elements has a small but significant effect, particularly for E^b.

The Marcus theory results are particularly interesting. Conventional Marcus theory (as in eq 1) is correctly able to predict barriers with good precision in some cases. However, in several of the cases (notably when SH^- or PH_2^- are involved), deviations of well over 5 kcal mol^{-1} for E^* are obtained. Marcus theory is heavily dependent upon the choice of reference for E^0. For example, should a backside complex be chosen even though it is not a stationary point on the potential energy surface? Thus, we investigated the use of collinear reference complexes for some of the barrier heights. This turned out not to be an improvement on the conventional Marcus results, with some deviations among the collinear data of over 10 kcal mol^{-1} for $E^*_{F,OH}$ and E^*_{F,NH_2}. Clearly, the use of collinear references is not the way to get higher accuracy. The performance of standard Marcus theory is a concern, considering the wide body of literature supporting its utilization.[24−26,58−60,62]

The augmented Marcus theory (as in eq 7), which is independent of the well depth, exhibits much higher precision. The augmented form has (average, maximum) deviations of (1.35, 2.52) kcal mol^{-1}, as compared with (3.50, 9.64) kcal mol^{-1} for conventional Marcus theory. This striking performance bodes well for the future use of this augmented form in predicting barriers. Further research should explore why conventional Marcus theory has such deviations, particularly when it appears that the large differences correspond to systems with second-row atoms (specifically S and P).

Finally, this research would not be complete without mention of possible improvements. Our previous manuscript[45] discussed the role of quadruple excitations on the energetics. We determined that quadruple excitations were only important when a particularly severe imbalance in the electronic structure of nucleophile and leaving group was present. Clearly, that is not a concern here. Still, the error bars associated with these energetics would decrease by 0.1−0.2 kcal mol^{-1} if correlation effects beyond CCSD(T) were included.

Acknowledgment. This research was supported by the U.S. National Science Foundation Grant CHE-0451445.

Supporting Information Available: Tables of geometries in internal coordinated, harmonic vibrational frequencies, and absolute energies for all structures at the RHF, B3LYP, BLYP, BP86, MP2, CCSD, and CCSD(T) levels of theory using DZP+dif, TZ2P+dif, and TZ2Pf+dif basis sets. All focal point absolute energies, along with core correlation and relativistic corrections. This material is available free of charge via the Internet at http://pubs.acs.org.

References and Notes

(1) Bohme, D. K.; Young, L. B. *J. Am. Chem. Soc.* **1970**, *92*, 7354.
(2) Bohme, D. K.; Mackay, G. I.; Payzant, J. D. *J. Am. Chem. Soc.* **1974**, *96*, 4027.
(3) Tanaka, K.; Mackay, G. I.; Payzant, J. D.; Bohme, D. K. *Can. J. Chem.* **1976**, *54*, 1643.
(4) Brauman, J. I.; Olmstead, W. N.; Lieder, C. A. *J. Am. Chem. Soc.* **1974**, *96*, 4030.
(5) Olmstead, W. N.; Brauman, J. I. *J. Am. Chem. Soc.* **1977**, *99*, 4219.
(6) Asubiojo, O. I.; Brauman, J. I. *J. Am. Chem. Soc.* **1979**, *101*, 3715.
(7) Pross, A.; Shaik, S. S. *New J. Chem.* **1989**, *13*, 427.
(8) DePuy, C. H.; Gronert, S.; Mullin, A.; Bierbaum, V. M. *J. Am. Chem. Soc.* **1990**, *112*, 8650.
(9) Wang, H. B.; Hase, W. L. *J. Am. Chem. Soc.* **1997**, *119*, 3093.
(10) Uggerud, E. *J. Chem. Soc. Perkin Trans. 2* **1999**, 1459.
(11) Viggiano, A. A.; Midey, A. J. *J. Phys. Chem. A* **2000**, *104*, 6786.
(12) Takeuchi, K.; Takasuka, M.; Shiba, E.; Kinoshita, T.; Okazaki, T.; Abboud, J. L. M.; Notario, R.; Castano, O. *J. Am. Chem. Soc.* **2000**, *122*, 7351.
(13) Davico, G. E.; Bierbaum, V. M. *J. Am. Chem. Soc.* **2000**, *122*, 1740.
(14) Baschky, M. C.; Kass, S. R. *Int. J. Mass Spectrom.* **2000**, *196*, 411.
(15) Su, T.; Wang, H. B.; Hase, W. L. *J. Phys. Chem. A* **1998**, *102*, 9819.
(16) Ervin, K. M. *Int. J. Mass Spectrom.* **1998**, *187*, 343.
(17) Tachikawa, H.; Igarashi, M. *Chem. Phys. Lett.* **1999**, *303*, 81.
(18) Li, G. S.; Hase, W. L. *J. Am. Chem. Soc.* **1999**, *121*, 7124.
(19) Raugei, S.; Cardini, G.; Schettino, V. *J. Chem. Phys.* **1999**, *111*, 10887.
(20) Tachikawa, H. *J. Phys. Chem. A* **2000**, *104*, 497.
(21) Yamataka, H. *Rev. Heteroat. Chem.* **1999**, *21*, 277.
(22) Okuno, Y. *J. Am. Chem. Soc.* **2000**, *122*, 2925.
(23) Dougherty, R. C.; Roberts, J. D. *Org. Mass Spectrom.* **1973**, *8*, 81.
(24) Pellerite, M. J.; Brauman, J. I. *J. Am. Chem. Soc.* **1980**, *102*, 5993.
(25) Pellerite, M. J.; Brauman, J. I. *J. Am. Chem. Soc.* **1983**, *105*, 2672.
(26) Dodd, J. A.; Brauman, J. I. *J. Phys. Chem.* **1986**, *90*, 3559.
(27) Lewis, E. S. *J. Phys. Chem.* **1986**, *90*, 3756.
(28) Hoz, S.; Basch, H.; Wolk, J. L.; Hoz, T.; Rozental, E. *J. Am. Chem. Soc.* **1999**, *121*, 7724.
(29) Shi, Z.; Boyd, R. J. *J. Am. Chem. Soc.* **1990**, *112*, 6789.
(30) Bickelhaupt, F. M.; Baerends, E. J.; Nibbering, N. M. M.; Ziegler, T. *J. Am. Chem. Soc.* **1993**, *115*, 9160.
(31) Deng, L.; Branchdell, V.; Ziegler, T. *J. Am. Chem. Soc.* **1994**, *116*, 10645.
(32) Glukhovtsev, M. N.; Pross, A.; Radom, L. *J. Am. Chem. Soc.* **1994**, *117*, 2024.
(33) Wladkowski, B. D.; Allen, W. D.; Brauman, J. I. *J. Phys. Chem.* **1994**, *98*, 13532.
(34) Gronert, S.; Merrill, G. N.; Kass, S. R. *J. Org. Chem.* **1995**, *60*, 488.
(35) Glukhovtsev, M. N.; Bach, R. D.; Pross, A.; Radom, L. *Chem. Phys. Lett.* **1996**, *260*, 558.
(36) Botschwina, P.; Horn, M.; Seeger, S.; Oswald, R. *Ber. Bunsen-Ges. Phys. Chem.* **1997**, *101*, 387.
(37) Botschwina, P. *Theor. Chem. Acc.* **1998**, *99*, 426.
(38) Bickelhaupt, F. M. *J. Comput. Chem.* **1998**, *20*, 114.
(39) Igarashi, M.; Tachikawa, H. *Int. J. Mass Spectrom.* **1998**, *181*, 151.
(40) Aida, M.; Yamataka, H. *J. Mol. Struct.* **1999**, *462*, 417.
(41) Mo, Y. R.; Gao, J. L. *J. Comput. Chem.* **2000**, *21*, 1458.
(42) Parthiban, S.; de Oliveira, G.; Martin, J. M. L. *J. Phys. Chem. A* **2001**, *105*, 895.
(43) Lee, I.; Kim, C. K.; Sohn, C. K.; Li, H. G.; Lee, H. W. *J. Phys. Chem. A* **2002**, *106*, 1081.
(44) Gonzales, J. M.; Cox, R. S.; Brown, S. T.; Allen, W. D.; Schaefer, H. F. *J. Phys. Chem. A* **2001**, *105*, 11327.
(45) Gonzales, J. M.; Pak, C.; Cox, R. S.; Allen, W. D.; Schaefer, H. F.; Tarczay, G.; Csaszar, A. G. *Chem.-Eur. J.* **2003**, *9*, 2173.
(46) Kuznetsov, A. M. *J. Phys. Chem. A* **1999**, *103*, 1239.
(47) Craig, S. L.; Brauman, J. I. *J. Am. Chem. Soc.* **1999**, *121*, 6690.

(48) Langer, J.; Matejcik, S.; Illenberger, E. *Phys. Chem. Chem. Phys.* **2000**, *2*, 1001.
(49) Saunders, W. H. *J. Org. Chem.* **2000**, *65*, 681.
(50) Ma, B. Y.; Kumar, S.; Tsai, C. J.; Hu, Z. J.; Nussinov, R. *J. Theor. Biol.* **2000**, *203*, 383.
(51) Jensen, H.; Daasbjerg, K. *J. Chem. Soc. Perkin Trans.* **2000**, *2*, 1251.
(52) Marcus, R. A. *J. Phys. Chem.* **1968**, *72*, 891.
(53) Cohen, A. O.; Marcus, R. A. *J. Phys. Chem.* **1968**, *72*, 4249.
(54) Kreevoy, M. M.; Oh, S. W. *J. Am. Chem. Soc.* **1973**, *95*, 4805.
(55) Kresge, A. J. *Chem. Soc. Rev.* **1973**, *2*, 475.
(56) Kreevoy, M. M.; Lee, I. S. *J. Am. Chem. Soc.* **1984**, *106*, 2550.
(57) Blowers, P.; Masel, R. I. *J. Phys. Chem. A* **1999**, *103*, 7047.
(58) Wolfe, S.; Mitchell, D. J.; Schlegel, H. B. *J. Am. Chem. Soc.* **1981**, *103*, 7694.
(59) Dodd, J. A.; Brauman, J. I. *J. Am. Chem. Soc.* **1984**, *106*, 5356.
(60) Lewis, E. S.; McLaughlin, M. L.; Douglas, T. A. *J. Am. Chem. Soc.* **1985**, *107*, 6668.
(61) Shi, Z.; Boyd, R. J. *J. Am. Chem. Soc.* **1991**, *113*, 2434.
(62) Wladkowski, B. D.; Brauman, J. I. *J. Phys. Chem.* **1993**, *97*, 13158.
(63) Marcus, R. A. *Annu. Rev. Phys. Chem.* **1964**, *15*, 155.
(64) Shaik, S. S.; Schlegel, H. B.; Wolfe, S. *Theoretical Aspects of Physical Organic Chemistry: The S_N2 Mechanism*; John Wiley & Sons Inc.: New York, 1991.
(65) Csaszar, A. G.; Allen, W. D.; Schaefer, H. F. *J. Chem. Phys.* **1998**, *108*, 9751.
(66) Irikura, K.; Frurip, D. J. *Computational Thermochemistry*; American Chemical Society: Washington, DC, 1998.
(67) Pople, J. A.; Head-Gordon, M.; Fox, D. J.; Raghavachari, K.; Curtiss, L. A. *J. Chem. Phys.* **1989**, *90*, 5622.
(68) Curtiss, L. A.; Jones, C.; Trucks, G. W.; Raghavachari, K.; Pople, J. A. *J. Chem. Phys.* **1990**, *93*, 2537.
(69) Curtiss, L. A.; Raghavachari, K.; Trucks, G. W.; Pople, J. A. *J. Chem. Phys.* **1991**, *94*, 7221.
(70) Curtiss, L. A.; Raghavachari, K.; Redfern, P. C.; Rassolov, V.; Pople, J. A. *J. Chem. Phys.* **1998**, *109*, 7764.
(71) Curtiss, L. A.; Redfern, P. C.; Rassolov, V.; Kedziora, G.; Pople, J. A. *J. Chem. Phys.* **2001**, *114*, 9287.
(72) Petersson, G. A.; Bennet, A.; Tensfeldt, T. G.; Al-Laham, M. A.; Shirley, W. A.; Mantzaris, J. *J. Chem. Phys.* **1988**, *89*, 2193.
(73) Ochterski, J. W.; Petersson, G. A.; Wilberg, K. B. *J. Am. Chem. Soc.* **1995**, *117*, 11299.
(74) Ochterski, J. W.; Petersson, G. A.; Montgomery, J. A. *J. Chem. Phys.* **1996**, *104*, 2598.
(75) Montgomery, J. A.; Ochterski, J. W.; Petersson, G. A. *J. Chem. Phys.* **1994**, *101*, 5900.
(76) Martin, J. M. L.; de Oliveira, G. *J. Chem. Phys.* **1999**, *111*, 1843.
(77) Boese, A. D.; Oren, M.; Atasoylu, O.; Martin, J. M. L.; Kállay, M.; Gauss, J. *J. Chem. Phys.* **2004**, *120*, 4129.
(78) Allen, W. D.; East, A. L. L.; Csaszar, A. G. *Structures and Conformations of Non-Rigid Molecules*; Kluwer: Dordrecht, 1993.
(79) East, A. L. L.; Allen, W. D. *J. Chem. Phys.* **1993**, *99*, 4638.
(80) King, R. A.; Allen, W. D.; Schaefer, H. F. *J. Chem. Phys.* **2000**, *112*, 5585.
(81) Bauschlicher, C. W.; Langhoff, S. R.; Taylor, P. R. *J. Chem. Phys.* **1988**, *88*, 2540.
(82) Bauschlicher, C. W.; Partridge, H. *J. Chem. Phys.* **1994**, *100*, 4329.
(83) Csaszar, A. G. *J. Phys. Chem.* **1994**, *98*, 8823.
(84) Csaszar, A. G.; Allen, W. D. *J. Chem. Phys.* **1996**, *104*, 2746.
(85) Martin, J. M. L. *Chem. Phys. Lett.* **1995**, *242*, 343.
(86) East, A. L. L.; Radom, L. *J. Mol. Struct.* **1996**, *376*, 437.
(87) Dyall, K. G.; Taylor, P. R.; Faegri, K.; Partridge, H. *J. Chem. Phys.* **1991**, *95*, 2583.
(88) Schwerdtfeger, P.; Laakkonen, L. J.; Pyykko, P. *J. Chem. Phys.* **1992**, *96*, 6807.
(89) Perera, S. A.; Bartlett, R. J. *Chem. Phys. Lett.* **1993**, *216*, 606.
(90) Balasubramanian, K. *Relativistic Effects in Chemistry, Part A: Theory and Techniques and Part B: Applications*; Wiley: New York, 1997.
(91) Cowan, R. D.; Griffin, D. C. *J. Opt. Soc. Am.* **1976**, *66*, 1010.
(92) Tarczay, G.; Csaszar, A. G.; Klopper, W.; Quiney, H. M. *Mol. Phys.* **2001**, *99*, 1769.
(93) Moller, C.; Plesset, M. S. *Phys. Rev.* **1934**, *46*, 618.
(94) Cizek, J. *J. Adv. Chem. Phys.* **1969**, *14*, 35.
(95) Purvis, G. D.; Bartlett, R. J. *J. Chem. Phys.* **1982**, *76*, 1910.
(96) Scuseria, G. E.; Janssen, C. L.; Schaefer, H. F. *J. Chem. Phys.* **1988**, *89*, 7382.
(97) Pople, J. A.; Head-Gordon, M.; Raghavachari, K. *J. Chem. Phys.* **1987**, *87*, 5968.
(98) Becke, A. D. *J. Chem. Phys.* **1993**, *98*, 5648.
(99) Lee, C.; Yang, W.; Parr, R. G. *Phys. Rev. B* **1988**, *37*, 785.
(100) Becke, A. D. *Phys. Rev. A* **1988**, *38*, 3098.
(101) Perdew, J. P. *Phys. Rev. B* **1986**, *33*, 8822.
(102) Dunning, T. H. *J. Chem. Phys.* **1989**, *90*, 1007.
(103) Kendall, R. A.; Dunning, T. H.; Harrison, R. J. *J. Chem. Phys.* **1992**, *96*, 6796.
(104) Woon, D. E.; Dunning, T. H. *J. Chem. Phys.* **1993**, *98*, 1358.
(105) Woon, D. E.; Dunning, T. H. *J. Chem. Phys.* **1994**, *100*, 2975.
(106) Woon, D. E.; Dunning, T. H. *J. Chem. Phys.* **1995**, *103*, 4572.
(107) Wilson, A. K.; van Mourik, T.; Dunning, T. H. *J. Mol. Struct.* **1996**, *388*, 339.
(108) Martin, J. M. L. *J. Chem. Phys.* **1998**, *108*, 2791.
(109) Martin, J. M. L.; Uzan, O. *Chem. Phys. Lett.* **1998**, *282*, 16.
(110) Bauschlicher, C. W.; Ricca, A. *J. Phys. Chem. A* **1998**, *102*, 8044.
(111) Tarczay, G.; Csaszar, A. G.; Leininger, M. L.; Klopper, W. *Chem. Phys. Lett.* **2000**, *322*, 119.
(112) Dunning, T. H.; Peterson, K. A.; Wilson, A. K. *J. Chem. Phys.* **2001**, *114*, 9244.
(113) Feller, D. *J. Chem. Phys.* **1993**, *98*, 7059.
(114) Tarczay, G.; Csaszar, A. G.; Polyansky, O. L.; Tennyson, J. *J. Chem. Phys.* **2001**, *115*, 1229.
(115) Frisch, M. J.; Trucks, G. W.; Schlegel, H. B.; Gill, P. M. W.; Johnson, B. G.; Robb, M. A.; Cheeseman, J. R.; Keith, T.; Petersson, G. A.; Montgomery, J. A.; Raghavachari, K.; Al-Laham, M. A.; Zakrzewski, V. G.; Ortiz, J. V.; Foresman, J. B.; Cioslowski, J.; Stefanov, B. B.; Nanayakkara, A.; Challacombe, M.; Peng, C. Y.; Ayala, P. Y.; Chen, W.; Wong, M. W.; Andres, J. L.; Replogle, E. S.; Gomperts, R.; Martin, R. L.; Fox, D. J.; Binkley, J. S.; Defrees, D. J.; Baker, J.; Stewart, J. P.; Head-Gordon, M.; Gonzalez, C.; Pople, J. A. *Gaussian 94*, revision C.3; Gaussian, Inc.: Pittsburgh, PA, 1995.
(116) Harrison, R. J.; Nichols, J. A.; Straatsma, T. P.; Dupuis, M.; Bylaska, E. J.; Fann, G. I.; Windus, T. L.; Apra, E.; de Jong, W.; Hirata, S.; Hackler, M. T.; Anchell, J.; Bernholdt, D. E.; Borowski, P.; Clark, T.; Clerc, D.; Dachsel, H.; Deegan, M.; Dyall, K. G.; Elwood, D.; Fruchtl, H.; Glendenning, E.; Gutowski, M.; Hirao, K.; Hess, A.; Jaffe, J.; Johnson, B.; Ju, J.; Kendall, R.; Kobayashi, R.; Kutteh, R.; Lin, J.; Littlefield, R.; Long, X.; Meng, B.; Nakajima, T.; Nieplocha, J.; Niu, S.; Rosing, M.; Sandrone, G.; Stave, M.; Taylor, H.; Thomas, G.; van Lenthe, J.; Wolinski, K.; Wong, A.; Zhang, Z. *NWChem, A Computational Chemistry Package for Parallel Computers*, Version 4.1; Richland, WA, 2002.
(117) Crawford, T. D.; Sherrill, C. D.; Valeev, E. F.; Fermann, J. T.; Leininger, M. L.; King, R. A.; Brown, S. T.; Janssen, C. L.; Seidl, E. T.; Yamaguchi, Y.; Allen, W. D.; Xie, Y.; Vacek, G.; Hamilton, T. P.; Kellog, C. B.; Remington, R. B.; Schaefer, H. F. *PSI 3.0*; PSITECH, Inc.: Watkinsville, GA, 1999.
(118) Vetter, R.; Zulicke, L. *J. Am. Chem. Soc.* **1990**, *112*, 5136.
(119) Shi, Z.; Boyd, R. J. *J. Am. Chem. Soc.* **1991**, *113*, 1072.
(120) Schlegel, H. B.; Mislow, K.; Bernardi, F.; Bottini, A. *Theor. Chim. Acta* **1977**, *44*, 245.
(121) Blavins, J. J.; Cooper, D. L.; Karadakov, D. B. *J. Phys. Chem. A* **2004**, *108*, 914.
(122) Okuno, Y. *Int. J. Quantum Chem.* **1998**, *68*, 261.
(123) Zhou, Z.; Zhou, X.; Fu, H.; Tian, L. *Spectrochim. Acta A* **2002**, *58*, 2061.
(124) Kormos, B. L.; Cramer, C. J. *J. Phys. Org. Chem* **2002**, *15*, 712.
(125) Yang, S. Y.; Fleurat-Lessard, P.; Hristov, I.; Ziegler, T. *J. Phys. Chem. A* **2004**, *108*, 9461.
(126) Ruggiero, G. D.; Williams, I. H. *J. Chem. Soc. Perkin Trans. 2* **2002**, 591.
(127) Riveros, J. M.; Sena, M.; Guedes, L. A. X.; Slepetys, R. *Pure Appl. Chem.* **1998**, *70*, 1969.
(128) Sun, L. P.; Song, K. Y.; Hase, W. L. *Science* **2002**, *296*, 875.
(129) June, Y. C.; Vande Linde, S. R.; Zhu, L.; Hase, W. L. *J. Chem. Phys.* **1992**, *96*, 8275.
(130) Vande Linde, S. R.; Hase, W. L. *J. Am. Chem. Soc.* **1989**, *111*, 2349.